Environmental Science & Technology

pubs.acs.org/est

Article

The PCOS–NAFLD Multidisease Phenotype Occurred in Medaka Fish Four Generations after the Removal of Bisphenol A Exposure

Sourav Chakraborty, Santosh Anand, Seraiah Coe, Beh Reh, and Ramji Kumar Bhandari*

Cite This: *Environ. Sci. Technol.* 2023, 57, 12602–12619

Read Online

ACCESS | Metrics & More | Article Recommendations | Supporting Information

ABSTRACT: As a heterogeneous reproductive disorder, polycystic ovary syndrome (PCOS) can be caused by genetic, diet, and environmental factors. Bisphenol A (BPA) can induce PCOS and nonalcoholic fatty liver disease (NAFLD) due to direct exposure; however, whether these phenotypes persist in future unexposed generations is not currently understood. In a previous study, we observed that transgenerational NAFLD persisted in female medaka for five generations (F4) after exposure to an environmentally relevant concentration (10 μg/L) of BPA. Here, we demonstrate PCOS in the same F4 generation female medaka that developed NAFLD. The ovaries contained immature follicles, restricted follicular progression, and degenerated follicles, which are characteristics of PCOS. Untargeted metabolomic analysis revealed 17 biomarkers in the ovary of BPA lineage fish, whereas transcriptomic analysis revealed 292 genes abnormally expressed, which were similar to human patients with PCOS. Metabolomic–transcriptomic joint pathway analysis revealed activation of the cancerous pathway, arginine–proline metabolism, insulin signaling, AMPK, and HOTAIR regulatory pathways, as well as upstream regulators *esr1* and *tgf* signaling in the ovary. The present results suggest that ancestral BPA exposure can lead to PCOS phenotypes in the subsequent unexposed generations and warrant further investigations into potential health risks in future generations caused by initial exposure to EDCs.

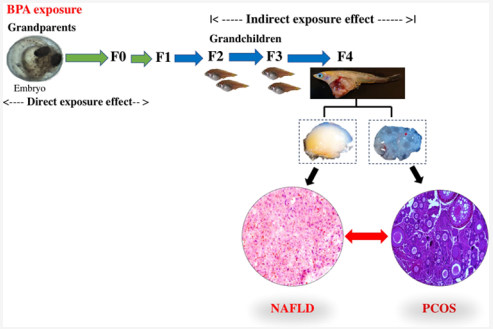

KEYWORDS: *bisphenol A, NAFLD, PCOS, medaka, transcriptome, metabolome, transgenerational inheritance*

1. INTRODUCTION

Since the middle of the 20th century, there has been substantial growth in the development and production of industrial chemicals. BPA is one of the most widely manufactured chemicals and an environmental contaminant worldwide. BPA can induce epigenetic alteration in germline stem cells and gametes.[1−3] Aside from causing adverse reproductive and nonreproductive health outcomes in the directly exposed generations, BPA can also contribute to transgenerational health outcomes in several subsequent generations.[4,5] Various BPA-induced transgenerational health effects have been reported in animal models, such as diminished fertilization rate[6,7] and osmoregulatory gene expression,[8] cardiac disorders,[9,10] social recognition and behavioral variations,[11] and reproductive and metabolic diseases.[5,12] Because of its widespread health effects, BPA has been banned in North America and the European Union in certain consumer goods.[13−15] Although BPA is currently banned, the current ban may not completely protect future generations' reproductive and metabolic health because ancestral BPA exposure-induced epigenetic changes in germ cells can be passed on to somatic cells of future generations, leading to impaired metabolic and reproductive health.[4,5] We have previously demonstrated that ancestral BPA exposure could cause transgenerational nonalcoholic fatty liver disease (NAFLD), which can persist for five generations in medaka.[16] In fish, the liver plays an intrinsic role in female reproduction by providing the major egg yolk precursor protein, i.e., vitellogenin, that supports embryo development and larvae by supplementing protein and lipid-rich nutrients.

Typically, ovarian function depends largely on the hypothalamus–pituitary–ovary (HPO) axis activated by GnRH pulsatility followed by releases of pituitary-derived gonadotropins such as follicle-stimulating hormone (FSH), luteinizing hormone (LH), and sex steroids (estrogen, progesterone, testosterone) secreted by gonads.[17,18] As the most common female reproductive disease, polycystic ovarian syndrome (PCOS) is characterized by an imbalance between FSH and LH, inhibited follicle maturation, formation of multiple small cysts due to degeneration of follicles, and an increase in free testosterone.[19,20] Up to 75% of women of reproductive age suffer from PCOS due to hormonal imbalance, making it the most prevalent endocrine disease

Received: March 27, 2023
Revised: July 17, 2023
Accepted: July 18, 2023
Published: August 15, 2023

https://doi.org/10.1021/acs.est.3c01922
Environ. Sci. Technol. 2023, 57, 12602–12619

among premenopausal women.[21] As an acute endocrine disruptor, BPA dysregulates FSH and LH levels followed by abnormal folliculogenesis,[22] hinders embryo implantation,[23] alters estrous cyclicity,[24] and upregulates AMH, causing an increase in the number of preovulatory follicles.[25] BPA is presumed to be an epigenetically toxic compound.[26] Aside from causing adverse health outcomes in the exposed generation, BPA can also contribute to transgenerational health outcomes through abnormal epigenetic changes in germ cells via germline transmission.[27,28] In a previous study, polycystic ovarian syndrome was positively correlated with metabolic diseases such as NAFLD[29] and deregulation of estrogen signaling,[30−32] suggesting cross talk between the hepato-ovarian axis. A positive correlation has been found between PCOS and biopsy-confirmed NAFLD[33−35] at an intragenerational level; however, whether this relationship is heritable at the transgenerational level is not currently understood. The proposed study further investigates this issue by incorporating phenotypic and omics approaches.

A multidisease phenotype can develop in organisms due to direct exposure to environmental chemicals; however, the mechanisms underlying such compounded adverse health outcomes are not clearly understood. Neither is it clearly understood whether such phenotypes persist in organisms in subsequent generations after the remediation of the environmental contamination. Using a multi-omics (integrated transcriptomics and metabolomics) approach, the present study examined heritable NAFLD−PCOS, a multidisease phenotype, in medaka fish whose ancestors were exposed to BPA during their first 15 days of life and never thereafter. Fish, such as medaka and zebrafish, serve as biomedical animal models to study human diseases, including NAFLD and PCOS.[36−40] Because of the conserved mechanism for processing epigenetic information in post-fertilization stage embryos and primordial germ cells with mice and humans, medaka becomes an ideal animal model to study the environmentally induced epigenetic inheritance of transgenerational disease phenotype.[39,41]

2. MATERIALS AND METHODS

2.1. Animal Care and Maintenance. The Hd-rR strain of medaka was used.[42] The exposure and procedure for handling fish and euthanization were approved by the Institutional Animal Care and Use Committee (IACUC) of the University of North Carolina Greensboro (#20-002). Adult medaka fish were maintained in 20 L glass aquaria on a light−dark cycle of 14:10 h with a recirculatory water system with an exchange of 25% water every 4 h at 26 ± 1 °C and fed three times a day with Otohime granular food and newly hatched brine shrimp (*Artemia* nauplii). Embryos were incubated in glass Petri dishes and larvae in 1 L tanks until they could feed and swim independently. The larvae at above 25 dpf stage were transferred to 5 gal glass tanks for rearing until end point measurement. For this study, 4 month old adult medaka females were used.

2.2. Chemical Exposure. Bisphenol A exposure can affect metabolic and reproductive health at various concentrations.[43−47] The present study is the downstream analytical part of a bigger transgenerational study. The concentration of BPA was selected after testing a dose−response curve, and the concentration of BPA selected was 10 μg/L, which is realistic with regard to the environmental concentration in many regions of the world.[48,49] The measured concentration of BPA was within <10% of the calculated concentration throughout the exposure period, and uptake was measured to be 20 pg/mg egg/day as previously described.[48,49] BPA exposure was initiated 8 h post fertilization stage (hpf) and continued until day 15 after fertilization (dpf) with a renewal of exposure once daily. BPA exposure was designed to include epigenetic reprogramming events in germ cells and to avoid epigenetic reprogramming of embryos that takes place between fertilization and blastula stages (8 hpf). After the BPA exposure was complete, the F0 generation (exposed individuals) and subsequent generations (offspring) were raised in clean water without exposure to BPA. The exposure window thus included a critical developmental window for sex determination and liver differentiation.[50] The use of initial BPA exposure (10 μg/L) at F0 generation was previously reported to cause NAFLD, fertilization defects, and increased embryo mortality in subsequent unexposed generations of medaka.[8,16,48]

2.3. Production of BPA-Exposed Transgenerational Offspring. Generation of the BPA-exposed transgenerational lines of medaka was previously described.[51] Briefly, following BPA exposure for 15 days, larvae were raised in clean water until they became adults, designated as F0 adults (intragenerational due to direct exposure to BPA). At 120 days postfertilization, all experimental medaka reached sexual maturity and spawned.[52] A total of six pairs of fish from the F0 generation were bred at 120 days postfertilization to produce F1 (intergenerational). The same mating methodology was used to produce subsequent generations up to F4 (the fifth generation, transgenerational).

2.4. Fecundity and Fertilization Efficiency of the F4 Fish. The fish from BPA-exposed and control lineages were bred in glass tanks at a ratio of three females and two males for 7 days. Each morning, eggs laid by females were collected and examined under a microscope to determine fecundity and fertilization status. Fecundity was calculated as the average number of eggs laid per female per day. Eggs were examined under a stereoscope to confirm fertilization according to the methods previously described.[53] A two-tailed *t* test was performed between the F4 generation of BPA lineage and the control group to determine statistical significance.

2.5. Tissue Sample Collection. To examine whether the BPA lineage fish develop PCOS-like syndrome in adulthood (120 dpf), 15 females from each group (BPA lineage and control lineage) were euthanized with MS-222 (250 mg/L). The ovary and liver of both groups were dissected, weighed, and divided into two halves. For RNA/DNA extraction, half of the ovary and liver were fixed in RNA/DNA shield solution (Zymo Research, CA) and the other half in Bouin's solution for histopathological analysis. Hepatosomatic index (HSI), gonadosomatic index (GSI), and body mass index (BMI) were calculated as liver weight (g) × 100/body weight (g), ovary weight (g) × 100/body weight (g),[54] and [body weight (g) − ovary weight (g)]/body length (cm^2), respectively. Visceral fat was collected to quantify adipose tissue (see Supporting Information). For histological examination, samples were embedded in low-temperature paraffin, sectioned at 5 μm thickness in a microtome, and stained with hematoxylin following optimized histological protocol.[16] To determine fat accumulation, liver samples from the control and BPA lineages were fixed in the Optimal Cutting Temperature (OCT) compound, sectioned in a cryotome at 15 μm thickness, and used for Oil Red O staining.

https://doi.org/10.1021/acs.est.3c01922
Environ. Sci. Technol. 2023, 57, 12602−12619

2.6. Ovary Phenotyping. On the basis of follicular development, the ovary of the medaka was categorized into five developmental stages according to the literature previously published.[55] Stage I contained primary follicles with intense basophilic cytoplasm with a peripherally located nucleus. Stage II contained cortical alveolar stage oocytes. Stage III contained yolk in vitellogenic oocytes with conspicuous zona radiata. Stage IV contained abundant yolk granules in late vitellogenic oocytes with peripheral migration of the germinal vesicle. Stage V contained mature stage oocytes without germinal vesicles, according to the published literature.[56] Developmental stages of the ovary were measured in both groups (BPA lineage and control), and the two-way analysis of variance was used to evaluate the significance of differences in different stages of folliculogenesis.

Hyperplasia of granulosa cells; thinning, invasion, and breakdown of the zona radiata; disintegration of the basal membrane; and absorption of vitellus are the characteristics of atretic follicles.[57] The ImageJ software was used to measure the follicular area. The atretic follicles from control and BPA-lineage fish were analyzed by measuring the follicular area using the ImageJ software. The reference value was taken from the mean area of the atretic follicles ($1p^2$) in the control ovaries. Atretic follicles with a diameter greater than $1p^2$ were considered as big atretic follicles. Blind tests were conducted by two different lab members to characterize different stages of folliculogenesis and atretic follicles. The results were consistent among all testers.

2.7. RNA-Seq. *2.7.1. Library Preparation, RNA Sequencing, and Data Analysis.* The ovaries of control and BPA lineage female fish (15 individuals from each lineage) were used for total RNA extraction by using a Quick RNA/DNA Miniprep Plus Kit (#D-7003, Zymo Research, CA, USA) according to the manufacturer's protocol as previously described.[58] RNA quality was tested by bleach gel electrophoresis,[59] and the quantity was determined by Nanodrop 2000 and Qubit (Thermo Fisher, Waltham, MA). The RNA of the ovary from three females was pooled as one biological replicate per group. Transcriptome libraries were prepared using a NEBNext Ultra II RNA Kit and the manufacturer's protocol. The libraries were sequenced on Illumina HiSeq X (Novogene Corporation, CA, USA) using a 150 bp paired-end sequencing strategy (short reads), producing 20−40 million reads per biological replicate.

The reads were first preprocessed with fastp 0.23.2,[60] an ultrafast all-in-one FASTQ preprocessor, which performs quality control, adapter trimming, quality filtering, per-read quality pruning, and many other operations with a single scan of the FASTQ data. The processed reads were then mapped to the medaka genome (Oryzias_latipes.ASM223467v1) using STAR 2.7.7a.[61] Finally, DESeq2 v1.34.0 was used to do the differential expression analysis.[62] GSEA analysis was done using the GSEA Preranked tool (GSEA v4.1).[63,64] For GSEA analysis, only genes showing twofold up- or downregulation were considered. The Gene Ontology (GO) enrichments were obtained using "C5: ontology gene sets" of the MSigDB collection.[65]

2.7.2. Comparative Analysis of the BPA Lineage Ovary Gene Set with the Human PCOS Patient Data Set. A predefined set of PCOS specific DEGs was obtained from public human patient data sets: GSE34526125, GSE10946126, and ArrayExpress accession number E-MEXP-3641127.[66−68] The DEGs (FDR 0.05 and Log2FC > 0.5) from the medaka ovary RNA-seq were compared with the PCOS patient data set.[66] Overlapping DEGs between BPA lineage and PCOS patient group were selected and illustrated by using VENNY (http://bioinfogp.cnb.csic.es/tools/venny/index.html). The PCOS-specific DEGs represented in the ovary of the BPA lineage group were used, and predicted pathways were constructed using ShinyGO 0.76.3.[69]

2.8. RT-qPCR. Total RNA was isolated from the ovary and liver of the F4 generation fish using a Quick RNA/DNA Miniprep Plus Kit (#D-7003, Zymo Research, CA, USA) according to the manufacturer's protocol involving *Dnase I* treatment of RNA as previously described.[58] The RNA was reconstituted in 20 μL of nuclease-free water (Zymo Research, CA, USA) followed by testing RNA integrity by bleach gel electrophoresis[59] and quantified by Qubit and Nanodrop 2000 (A260/280 between 1.8 and 2). Reverse transcription of 1 μg of total RNA was performed on each sample using a high-capacity reverse transcription kit (Applied Biosciences) according to the manufacturer's instructions as previously described.[53,70] RT-qPCR was performed in a QuantStudio 3 Real-time PCR equipment (Applied Biosystems) using gene-specific primers (Table S1) and the $2^{-\Delta\Delta Ct}$ method. The *rpl7* gene was selected as a stable housekeeping gene after testing the expression pattern of several housekeeping genes. Primers were designed using Primer3web[71] from exon−exon junctions to avoid genomic DNA amplification (Table S1).

2.9. Ingenuity Pathway Analysis (IPA) of DEGs. Canonical pathways were determined by using the IPA software (V01-07; Qiagen), and molecular and cellular function were determined using the specific Ingenuity Knowledge Database (using default parameters for all tissues and cell lines, with relaxed filters), which provides a repository of biological interactions and functional annotations. Dysregulated genes (FDR 0.05 and Log2FC > 0.5) in the ovary of F4 generation fish were converted to the corresponding human orthologous using the g-profiler website.[72] Fisher's exact test was applied to calculate the significance of each network.

2.10. Metabolomic Quantification. The ovaries of F4 females from control and BPA lineage were pooled respectively and used to extract ovarian metabolites. According to a published protocol,[73] ovary samples (20 mg) were homogenized in an ultrasonically extracted solution consisting of methanol/acetonitrile/water (2:2:1, v/v), vortex mixed, and ultrasonically extracted twice at a low temperature for 30 min. After incubation at −20 °C for 1 h, the mixture was centrifuged at 13,000 rpm at 4 °C for 15 min. The supernatant was lyophilized and stored at −80 °C. Before use, the lyophilized sample was dissolved in acetonitrile water (1:1, v/v), vortex-mixed, and centrifuged at 14,000 rpm for 15 min. The supernatant was injected into the HPLC−MS/MS system for metabolomic analysis. To ensure the system's stability, eight quality control (QC) samples, including whole adductor muscle tissues, were inserted throughout the experiment. Mass spectrometry was performed on a Q Exactive plus (Thermo Fisher Scientific, Waltham, MA, USA) equipped with electrospray ionization. The mass spectrometry operational protocol was previously published.[74] Both negative and positive ion modes were applied with a capillary voltage setting of ±5.5 kV during instrument operations. The product ion scan m/z range was 25−1200 Da with a scan accumulation time of 0.03 s/spectrum. The collision energy was set to 30 eV.

2.11. Metabolomic Data Analysis. Mass spectrometric data were analyzed, aligned, and filtered with the MZmine 2.2

https://doi.org/10.1021/acs.est.3c01922
Environ. Sci. Technol. 2023, 57, 12602−12619

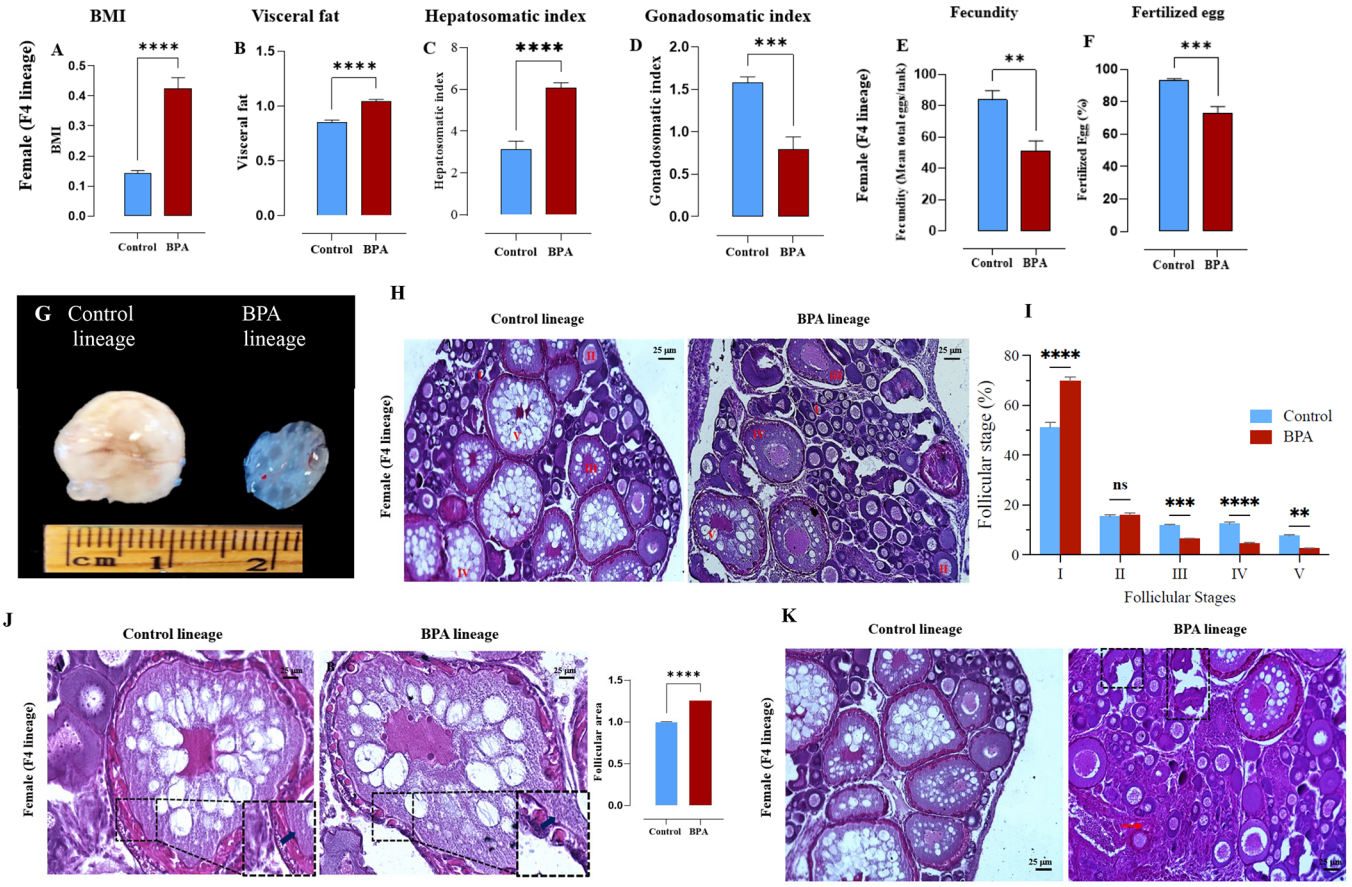

Figure 1. Ancestral BPA exposure caused increased basal metabolic index (BMI), visceral fat accumulation, and hepatosomatic index and reduced gonadosomatic index in BPA lineage females. (A) BMI (mass/length^2), (B) visceral fat, (C) hepatosomatic index, and (D) gonadosomatic index. Statistical significance (***$P < 0.001$, t test) compared to control lineage. Ancestral BPA exposure perturbed maturation of ovarian follicles with fertilization defect. (E) Fecundity, (F) fertilized egg, and (G) size of the ovary. (H) Ovary histology (magnification ×40) micrograph in control and BPA lineage. (I) Number of follicles in each developmental stage in the ovaries of the BPA and control lineage fish. Asterisks indicate statistically significant differences (***$P < 0.001$, t test). I: primary growth stage; II: cortical alveolar stage; III: early vitellogenic stage; IV: late vitellogenic stage; V: mature stage; A: atretic follicle. (J) Degenerated follicle (black rectangle) with excess interstitial tissue deposition (red arrow) found in the ovaries of BPA lineage fish. (K) Atretic follicle with damaged chorion found in the ovary of BPA lineage (magnification ×40) and follicular area.

software (http://mzmine.sourceforge.net/) using the procedure previously reported elsewhere.[74] Quantile normalization, cube root transformation, and mean centering were used to process the filtered peaks from 4232 peaks in the positive mode and 3569 peaks in the negative mode. The resulting features were used to explore the total pathway hit by the Mummichog algorithm installed in Metaboanalyst 5.0.[75] Metabolites associated with pathways were further used for PCA to reveal intrinsic feature clusters and detect outliers. To examine the relationship between group and spectral data with variance (R2Y) and predictive ability (Q2 parameter), a PLS-DA model was used. The resonance of metabolites was putatively annotated bioinformatically by using the HMDB database[76] (http://www.hmdb.ca) and metlin[77] (http://metlin.scripps.edu). To visualize the variations of metabolites between the control and BPA lineage group, the significantly altered metabolites in the BPA lineage compared with the control lineage were identified based on the following criteria: $P < 0.05$ and fold change $\geq \pm 1$. VIP > 1 was used for hierarchical clustering (Ward clustering, Euclidean distance), univariate analysis t test, and pathway analysis using Metaboanalyst 5.0 as previously described.[78] To determine metabolomic biomarkers of PCOS, the classical univariate ROC curve analysis was performed.[79] The area under the curve (AUC) was generally between 0.5 and 1.0. When AUC > 0.5 and closer to 1, the model performs better.[80] However, biomarkers were selected based on strict criteria: $P < 0.05$ and AUC = 1 from the ovary of the BPA lineage. BPA lineage ovary metabolites were compared with the PCOS patient metabolite data set.[81] The abundance of amino acids in the BPA lineage ovary was plotted in metabolic pathways associated with polycystic ovary syndrome (PCOS).[82]

2.12. Statistical Analysis. The GraphPad Prism (GraphPad Software, San Diego, CA) software was used for statistical analysis and plotting the results. Comparison of data between BPA lineage and control lineage, Student's t test, one-way analysis of variance (ANOVA), and post hoc multiple comparison tests (Tukey HSD) were used to determine significant differences. Differences with $P < 0.05$ were considered significant and have been marked with asterisks (*$P < 0.05$; **$P < 0.01$; ***$P < 0.001$).

3. RESULTS

3.1. F4 Generation Female Fish from the BPA-Exposed Lineage Showed Altered Morphological End Points. Body mass index (BMI) and gonadosomatic index (GSI) were measured to determine the metabolic health of the F4 females. Compared to the control lineage, the BPA lineage

https://doi.org/10.1021/acs.est.3c01922
Environ. Sci. Technol. 2023, 57, 12602−12619

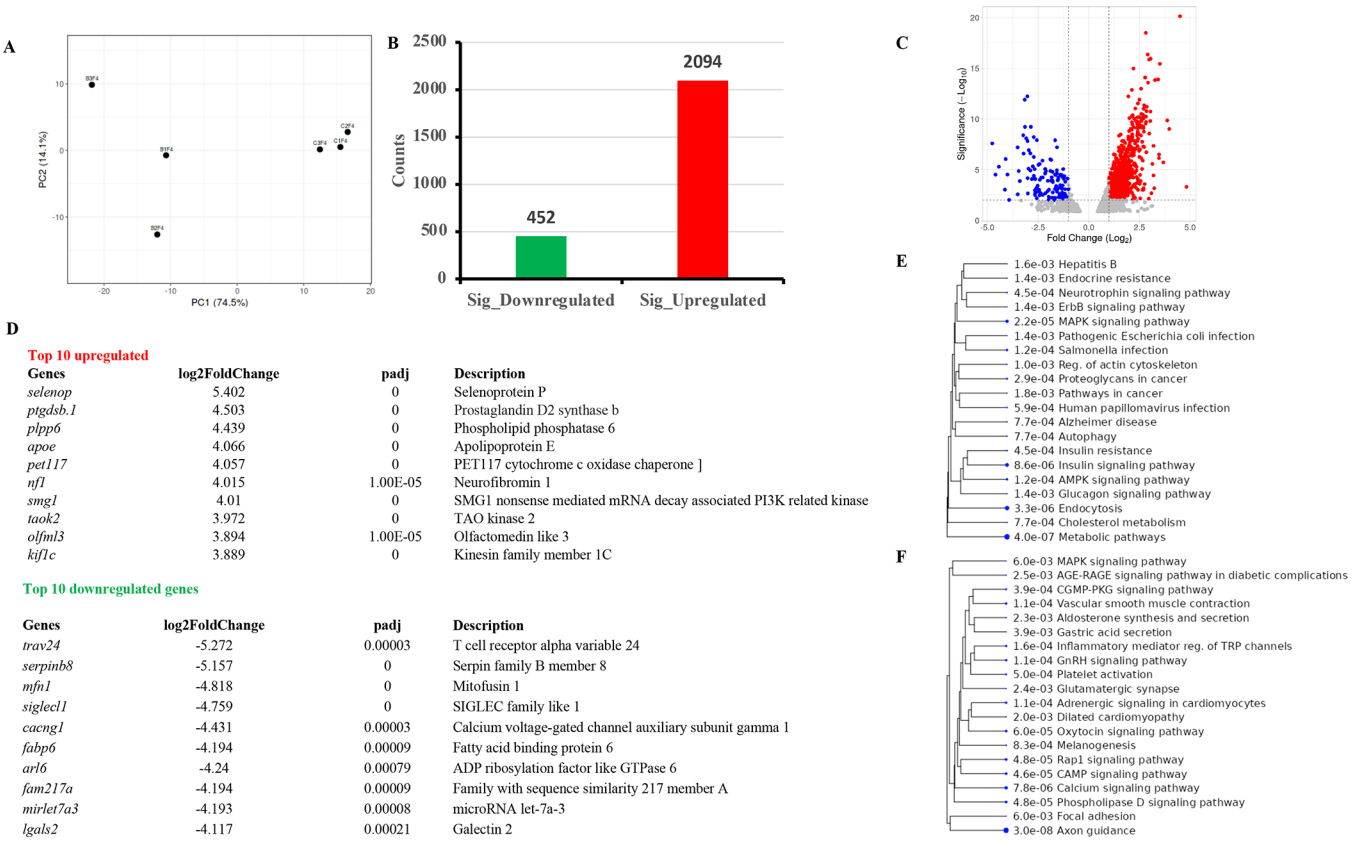

D

Top 10 upregulated

Genes	log2FoldChange	padj	Description
selenop	5.402	0	Selenoprotein P
ptgdsb.1	4.503	0	Prostaglandin D2 synthase b
plpp6	4.439	0	Phospholipid phosphatase 6
apoe	4.066	0	Apolipoprotein E
pet117	4.057	0	PET117 cytochrome c oxidase chaperone]
nf1	4.015	1.00E-05	Neurofibromin 1
smg1	4.01	0	SMG1 nonsense mediated mRNA decay associated PI3K related kinase
taok2	3.972	0	TAO kinase 2
olfml3	3.894	1.00E-05	Olfactomedin like 3
kif1c	3.889	0	Kinesin family member 1C

Top 10 downregulated genes

Genes	log2FoldChange	padj	Description
trav24	-5.272	0.00003	T cell receptor alpha variable 24
serpinb8	-5.157	0	Serpin family B member 8
mfn1	-4.818	0	Mitofusin 1
siglecl1	-4.759	0	SIGLEC family like 1
cacng1	-4.431	0.00003	Calcium voltage-gated channel auxiliary subunit gamma 1
fabp6	-4.194	0.00009	Fatty acid binding protein 6
arl6	-4.24	0.00079	ADP ribosylation factor like GTPase 6
fam217a	-4.194	0.00009	Family with sequence similarity 217 member A
mirlet7a3	-4.193	0.00008	microRNA let-7a-3
lgals2	-4.117	0.00021	Galectin 2

Figure 2. Global transcriptional alterations in the ovary. (A) PCA plot showing a separation of DEGs in BPA from control lineage ovaries. (B) Bar plots showing the profile of up- and downregulated genes and (C) log2 fold-change volcano plot. (D) Top 10 up- and downregulated genes in the ovary of BPA lineage. KEGG pathway analysis of total upregulated (E) and downregulated (F) genes in the transcriptome dataset.

females had significantly increased BMI, visceral fat content (Figure 1A,B), and hepatosomatic index (Figure 1C). However, the GSI (Figure 1D) was significantly decreased, suggesting that the F4 fish from the BPA lineage had a reproductive impairment.

3.2. Ancestral BPA Led to Altered Reproductive Outcomes in Females. To determine whether the females had reproductive defects, fecundity was measured, which accounts for the production of eggs per female in the BPA and control lineage. The mean total production of eggs per tank (fecundity) and the number of fertilized eggs were significantly decreased ($P < 0.05$) in the BPA lineage group compared to the control group (Figure1E,F). A 40% decrease in ovary size was observed in the BPA lineage fish (Figure 1G) compared to the control lineage. The number of vitellogenic and postvitellogenic follicles was significantly decreased in the BPA lineage (Figure 4A,B) except for stage II (Figure 1H). Overall, a 90% decrease in the number of vitellogenic and postvitellogenic follicles was observed. Morphometric analysis of the follicular stages showed a significantly higher number of stage I oocytes in the ovary of the BPA lineage fish, which decreased across stages III through stage V (Figure 1J). This indicated that follicular progression was disrupted in the BPA lineage fish. Furthermore, the BPA lineage group showed damage in the chorion (Figure 1J) and an increased mean area of atretic follicles (3.067 ± 0.6190 p^2, Figure 1J). Additionally, increased numbers of the atretic follicles, irregular folding of the surface epithelium, degenerated follicles with abnormal tissue deposition (Figure 1K), and hyperplasia of the granulosa cells were found in the ovary, indicating a loss of follicular architecture in BPA lineage fish.

3.3. Global Transcriptomic Alterations and GO Analysis in the Ovary. Principal component analysis (PCA) was able to separate 74.5% of biological replicates of both the BPA lineage and control lineage group into two clusters (Figure 2A), indicating that they are different from each other. The expression profiles were consistent across all three biological replicates, indicating that sequencing libraries were of excellent quality. In total, 2546 differentially expressed genes (DEGs), including 2094 upregulated and 452 downregulated genes, were identified in the BPA lineage group (Figure 2B), as exhibited in the volcano plot (Figure 2C). Global alterations in gene expression in BPA lineage ovary are illustrated in a heatmap (Figure S1). The GO analysis was performed to evaluate the functional properties of DEGs. GO results showed the top 20 molecular functions, biological processes, and cellular components (Figure S2). Among all biological processes, cellular morphogenesis, differentiation, and protein localization were highly enriched by DEGs from the BPA lineage. Cellular components and molecular function had DEGs involved in microtubule organization, cellular adhesion, and cellular transport mechanism via the Golgi apparatus. Additionally, using stricter selection criteria (fold change ≥ 2, p-adj ≤ 0.01), the top 10 up- and downregulated DEGs (biomarker) were selected from the BPA lineage group (Figure 2D). Most upregulated genes were enriched in insulin signaling pathway (Figure 2E, Figure S3), MAPK signaling (Figure 2E, Figure S4), AMPK signaling pathway (Figure 2E, Figure S5), and autophagy pathway (Figure 2E). Alternatively,

https://doi.org/10.1021/acs.est.3c01922
Environ. Sci. Technol. 2023, 57, 12602−12619

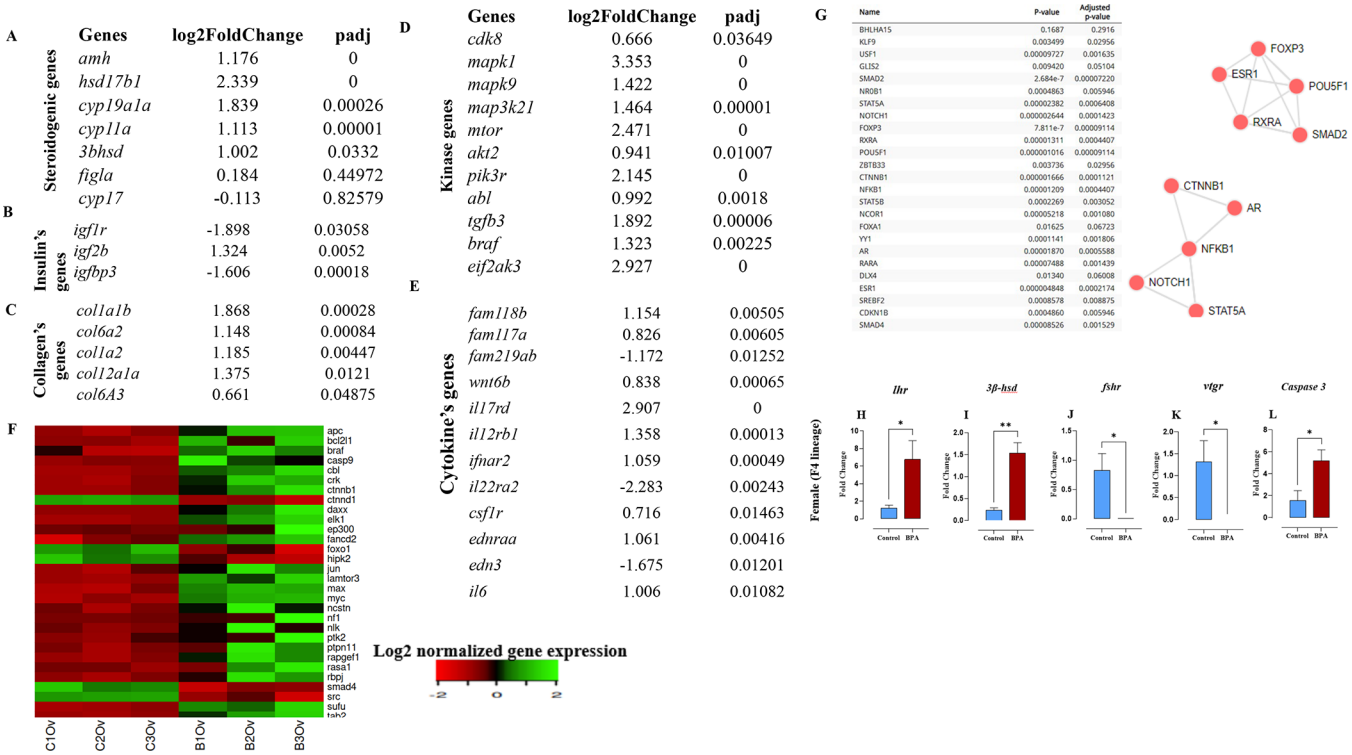

Figure 3. Abnormality in the expression of genes encoding (A) steroidogenic metabolism, (B) insulin signaling, (C) collagen synthesis, (D) kinase, (E) cytokine, and (F) cancerous genes. (G) List of significant transcription factors and their network in the ovary of the BPA lineage fish. Transcriptional alterations in gonadotrophin receptor genes in the ovaries of the BPA lineage fish. A significant increase in (H) *lhr* and (I) *3β-hsd* transcripts was observed in the BPA lineage ovaries. A significant decrease in (J) *fshr* and (K) *vtgr* transcript levels was found in the BPA lineage. A significantly abundant transcript of (L) *caspase 3* was measured in the BPA lineage ovaries. Asterisk indicates statistical significance at the level of $*P < 0.05$, *t* test compared against control lineage.

downregulated genes were enriched in Rap1 (Figure 2F, Figure S6), cAMP (Figure 2F, Figure S7), and AGE-RAGE signaling pathway (Figure 2F, Figure S7).

3.3.1. Gene Set Enrichment Analysis (GSEA) of Ovary Transcriptome. GSEA found a positive correlation of upregulated genes with autophagic mechanism (Figure S8A), cellular stress response (Figure S8B), and chromatin organization (Figure S8C). Downregulated DEGs were uniquely enriched with the cell signaling part of the biological pathway (Figure S8D). Additionally, DEGs were enriched with the cell cycle (Figure S9A), catabolic process (Figure S9FB), plasma membrane component (Figure S9C), mitochondria metabolic pathway (Figure S9D), apoptosis (Figure S9E), and p53 pathway (Figure S9F).

3.3.2. Aberrant Expression of Genes Encoding Transcription Factors, Collagen Synthesis, Cytokine, Kinase, Insulin Signaling Pathway, and Oncogenic Genes in the Ovary. Expression patterns of the genes that are associated with ovarian steroidogenic functions, including *amh*, *hsd17b1*, *cyp19a1*, *cyp11a1*, *3β-HSD*, and *cyp17*, were examined. RNA-seq results showed a significant upregulation of *Cyp11a1*, *amh*, *hsd17b1*, *3β-HSD*, *Cyp19a1* and a significant downregulation of *cyp17* in the BPA lineage group (Figure 3A). The expression of *igf1r* and *igfbp3* was downregulated, whereas *igf2b* expression was significantly upregulated, suggesting abnormal insulin signaling in the ovary (Figure 3B). The expression of genes encoding collagen proteins, mainly *col1a1b*, *col1a2*, and *col12a1*, was significantly upregulated (Figure 3C). This suggests abnormal tissue deposition in the ovary of the BPA linage. In the BPA lineage, specific genes encoding kinases, including *mapk1*, *mapk9*, *mtor*, *pik3r*, and *eif2ak3*, and cytokines, including *il17rd*, *il12rb1*, and *fam118b*, were significantly upregulated. However, the expressions of *il22ra2*, *fam219ab*, and *edn3* were significantly downregulated (Figure 3D,E). Abnormal expression of gene-encoding kinase and cytokine indicates molecular pathogenicity. The expressions of genes involved in malignancy such as *myc*, *akt1*, *apc*, *mtor*, *bcl2l1*, *daxx*, and *jun* were significantly upregulated, and only *smad4* and *src* genes were downregulated in the ovary of the BPA lineage group (Figure 3F). Additionally, essential transcription factors, such as *esr1*, *foxp3*, *smad 2*, *ar*, nfkb1, nothch1, klf9, and stat5 involved in the disease pathway were also identified (Figure 3G).

3.3.3. Alterations in the Expression of Reproductive Genes, Apoptosis Genes, and Genes Encoding Vitellogenin Receptors in the Ovary of the BPA Lineage. The mRNA levels of *lhr* ($P < 0.05$, Figure 3H) and *3β-hsd* ($P < 0.01$, Figure 3I) were significantly increased in the ovary of the BPA lineage. However, mRNAs of *fshr* ($P < 0.05$, Figure 3J) and *vtgr* ($P < 0.05$, Figure 3K) were significantly decreased in the ovary of the BPA lineage group. This indicated transgenerational dysregulation of steroidogenesis and reproduction-related pathways in the BPA lineage fish. Additionally, the levels of *caspase3* mRNAs were significantly increased ($P < 0.05$, Figure 3L) in the ovary of the BPA lineage, suggesting increased apoptosis-mediated cell death in the ovary of the BPA lineage fish.

3.3.4. DEGs of the F4 BPA Lineage PCOS Fish Overlapped with Those of the Human PCOS Patients. DEGs of BPA lineage PCOS fish were compared with publicly available

https://doi.org/10.1021/acs.est.3c01922
Environ. Sci. Technol. 2023, 57, 12602−12619

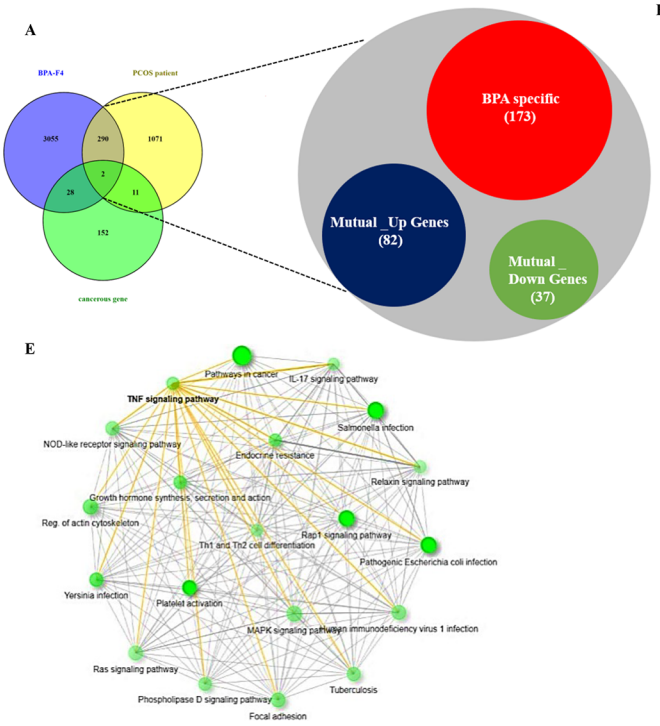

B

log2FoldChange		
Up_genes	BPA lineage	PCOS patient
myo5b	3.874	3.359
rab9b	3.735	2.452
atp2c1	2.918	2.316
il17rd	2.907	2.478
fam13c	2.753	2.864
col1a1	2.703	3.353
pard3b	2.518	3.471
frmd6	2.517	2.050
cox15	2.498	2.233
lrp6	2.482	2.223
ak4	2.436	2.074
sh3rf1	2.274	2.036
ar	2.197	2.381
gucy1a2	2.135	2.727
c5orf24	2.098	2.242

C

log2FoldChange		
Down_genes	BPA lineage	PCOS patient
lgals2	-4.117	-2.252
tmc6	-2.735	-2.184
cyth4	-2.557	-3.900
icam3	-2.466	-3.474
pecam1	-2.395	-5.506
tnfrsf1b	-2.268	-4.540
adgrg3	-1.923	-2.556
slc2a3	-1.902	-2.474
ptprg	-1.711	-2.556
magi1	-1.564	-2.000
tspan2	-1.489	-2.644
cyth1	-1.482	-2.059
emilin2	-1.461	-2.943
chst15	-1.418	-4.012
pde4a	-1.403	-2.252

D

log2FoldChange		
BPA specific	BPA lineage	PCOS patient
slc16a1	-3.232	2.025
kitlg	-3.127	3.020
ank3	-3.096	2.660
prss35	-2.618	3.159
slc1a3	-2.59	2.167
layn	-2.477	2.128
stc1	-2.273	2.553
loxl2	-2.115	3.079
glis2	-2.084	2.036
thap6	-1.928	2.585
psme4	-1.886	2.104
wasf3	-1.844	3.230
igfbp3	-1.606	2.759
eno2	-1.418	2.452
nt5e	-1.406	2.746

Figure 4. Comparison of DEGs found in the PCOS patient data set with those in the ovaries of BPA lineage fish. (A) An intersection of the Venn diagram showing common DEGs. (B) Top 15 mutually upregulated DEGs. (C) Top 15 mutually downregulated DEGs. (D) Top 15 mutual BPA-specific DEGs and (E) KEGG pathway enrichment on common DEGs.

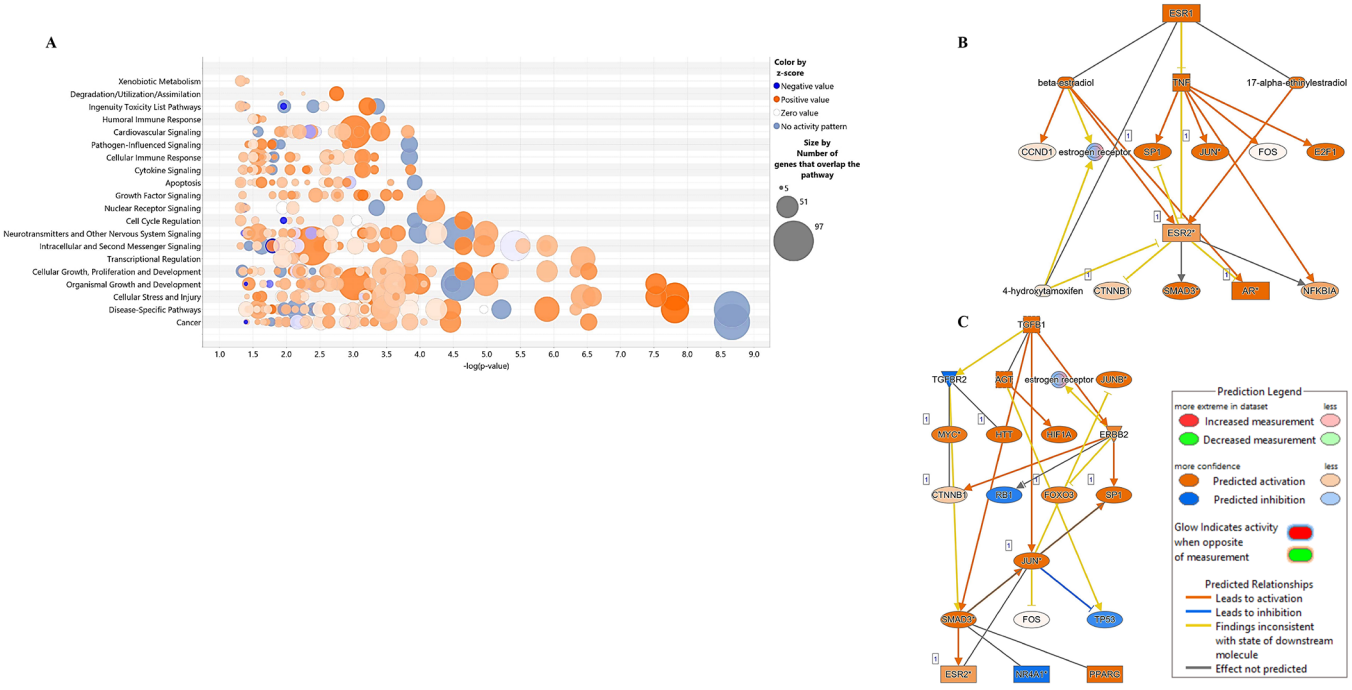

Figure 5. IPA analysis on the DEGs in the BPA lineage ovaries. (A) Canonical pathway. Upstream regulator gene networks within the DEGs determined by IPA. (B) ESR1 and (C) TGFB1 with interactive networks with downstream genes in the development of ovary pathogenesis.

human PCOS patient DEGs to identify end-point specific (PCOS) DEGs associated with ancestrally induced PCOS (end point) in the F4 generation.[66] In total, 292 common DEGs were found from the total of 1374 DEGs found in the human PCOS patient data set (Figure 4A). Additionally, 82 DEGs were mutually upregulated in both BPA lineage and PCOS patients. Among the total shared DEGs in BPA and PCOS patient groups, 37 DEGs were mutually downregulated. However, 173 shared DEGs showed exclusive expression patterns in the BPA lineage (Figure 4A). From the total shared DEGs, the top 15 mutually upregulated (Log2FC > 2), downregulated (Log2FC < −1), and exclusive BPA-specific DEGs are illustrated (Figure 4B−D). Heatmaps show shared common total DEGs between BPA lineage and PCOS patients

https://doi.org/10.1021/acs.est.3c01922
Environ. Sci. Technol. 2023, 57, 12602−12619

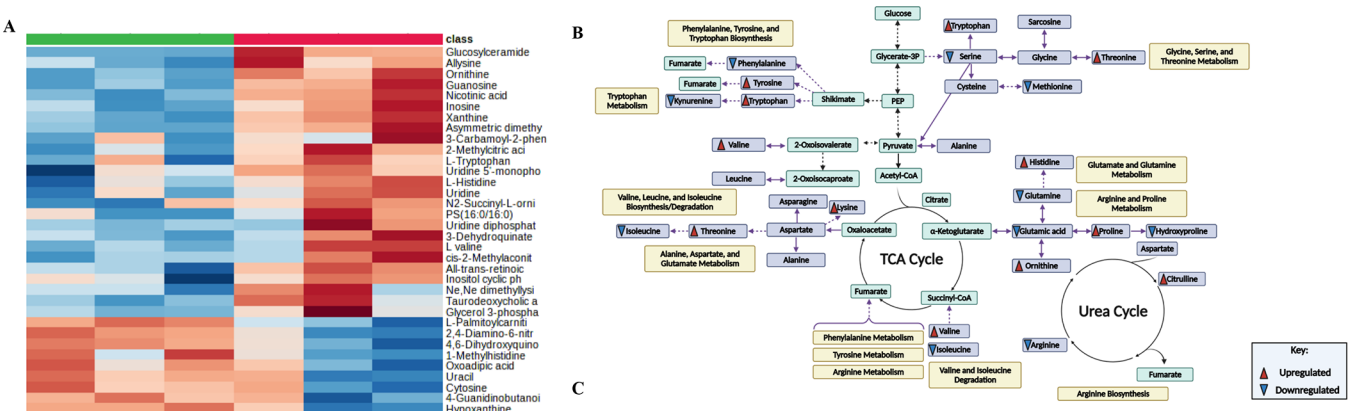

Biomarkers	AUC	p-value	Foldchange
Inosine	1	0.014579	1.003
Guanosine	1	7.19E-03	0.88543
Phosphocreatine	1	0.024705	-2.3582
2-Methylcitric acid	1	0.045657	0.77406
Taurodeoxycholic acid	1	0.024812	3.123
2,4-Diamino-6-nitrotoluene	1	0.036395	-1.4182
L-Palmitoylcarnitine	1	0.034512	-1.3656
Xanthine	1	0.006192	1.3
Niacinamide	1	0.003634	-1.5115
Asymmetric dimethylarginine	1	0.005527	0.92504
All-trans-retinoic acid	1	0.021409	1.019
Hypoxanthine	1	0.054476	-0.78665
Nicotinic acid	1	0.008282	1.1616
Ornithine	1	0.003527	1.8809
6-(alpha-D-Glucosaminyl)-1D-myo-inositol	1	0.008726	-2.1901
Glucosylceramide	1	0.000998	3.4792
Allysine	1	0.022583	0.90319

Figure 6. Global metabolic alterations in the ovary of BPA lineage fish. (A) Heatmap showing a differential abundance of the top 50 significant metabolites. (B) The abundance profile of amino acids in the PCOS metabolic pathway. (C) Table of biomarkers and the list of ovarian metabolites.

(Figure S10A−D). The comparative analysis revealed that the BPA lineage ovaries have similar gene expression patterns to human PCOS patients. KEGG pathway analysis on 292 DEGs showed significant enrichment in TNF signaling, IL signaling, growth hormone synthesis, and regulation of the actin cytoskeleton (Figure 4E). The transcriptome database has been submitted to NCBI as GSE226322 (token # qtqrqoycjtqfxqb).

3.3.5. IPA and Upstream Regulator Analysis. To further understand the biological pathway involved in diseased phenotype induced by ancestral BPA exposure, the RNA-seq data were annotated into human IDs for core functional analysis using IPA. Canonical pathways enriched in the molecular mechanism of cancer (*P* value 2.15E-09), autophagy (*P* value 2.95E-08), HOTAIR regulatory pathway (*P* value 3.00E-07), cellular stress and injury, cell cycle and transcriptional regulation, apoptosis, cytokine signaling, and immune response were determined (Figure 5A). DEGs were involved in the molecular mechanism of cancer (Figure S11), autophagy (Figure S12), and HOTAIR (Figure S13). Additionally, the gene-disease network analysis showed that *akt1* and *tnf* are master regulators of various disease pathways, such as HOTAIR regulatory pathways, AMPK signaling, growth failure, and autophagy, which are all indicative of severe ovarian disease due to ancestral BPA exposure (Figure S14). Using the upstream regulator analysis (URA) tool, IPA can identify potential upstream regulators by analyzing linkage to DEGs via coordinated expression.[83] A total of 94 transcription regulators were identified, and the top 15 transcription regulators were determined (Figure S15). *esr1* (estrogen receptor1) and *tgfb1* (transforming growth factor beta 1) were the most significant upstream regulators interacting with several genes such as *jun*, *myc*, *foxo3*, *smad3*, and *e2f1* (Figure 5B,C).

A. A Shift in Global Metabolites and Pathway Enrichment in the Ovary. Metabolomic analysis was conducted to address the alterations in ovarian metabolic profiles due to ancestral BPA exposure effect in the BPA-exposed control lineage group. An orthogonal partial least square discriminant analysis (OPLS-DA) was performed to elucidate the differences between the BPA and the control lineage group. According to the score plot, there was a difference among the groups (Figure S16). In this OPLS-DA model, R2X = 0.29, R2Y = 0.91, Q2 = 0.5. Metabolites with VIP > 1 are shown in Figure S17 with *m*/*z*, retention time, and HMDB class and IDs. The clustered heatmap showed the top 50 significant metabolites and their relative abundance (Figure 6A), providing useful insights into the relationship between unique metabolites of the BPA lineage and control lineage. The metabolites belonged to amino acids, purine and pyrimidine derivatives, organic acids, lipid molecules, sugars, and some other class of molecules. Lipid molecules such as glucosylceramide; PS (16:0/16:0); amino acids mainly L-histidine, allysine, L-tryptophan, and L-valine; and purine derivatives mainly guanosine, xanthine, hypoxanthine, and guanine were found in higher abundance in BPA lineage group. 4,6-Dihydroxyquinoline, vitamin K1 2,3-epoxide, uracil, phosphocreatine, cytosine, and L-aspartic acid were detected but in low abundance. Differential abundance of amino acids from the ovary of the BPA lineage fish was mapped in

https://doi.org/10.1021/acs.est.3c01922
Environ. Sci. Technol. 2023, 57, 12602−12619

A

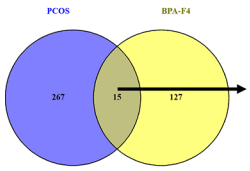

Mutual abundance pattern	PCOS	BPA-F4
Pregnenolone	↓	↓
Eicosapentaenoic acid	↑	↑
Phytosphingosine	↓	↓
Azelaic acid	↑	↑
Sphinganine	↓	↓
Phenylpyruvic acid	↑	↑
Ornithine	↑	↑
Inosine	↑	↑
Exclusive abundance pattern	**PCOS**	**BPA-F4**
Creatinine	↑	↓
Ceramide	↓	↑
Taurine	↑	↓
Pyroglutamic acid	↑	↓
Hypoxanthine	↑	↓
Uridine	↓	↑
Fructose 6-phosphate	↓	↑
Pantothenic acid	↑	↓

B

Transcriptome and Metabolomics Joint pathways	Total	Expected	Hits	Raw p	FDR
1 ABC transporters	183	9.0952	29	2.54E-08	7.26E-06
2 Central carbon metabolism in cancer	106	5.2682	21	4.39E-08	7.26E-06
3 Arginine biosynthesis	44	2.1868	12	9.88E-07	0.000109
4 Arginine and proline metabolism	128	6.3616	20	4.72E-06	0.000343
5 Aminoacyl-tRNA biosynthesis	118	5.8646	19	5.18E-06	0.000343
6 Protein digestion and absorption	142	7.0575	20	2.31E-05	0.001273
7 beta-Alanine metabolism	63	3.1311	12	5.26E-05	0.002489
8 Alanine, aspartate and glutamate metabolism	64	3.1808	12	6.19E-05	0.002561
9 Lysosome	127	6.3119	16	0.000543	0.019966
10 Insulin signaling pathway	141	7.0078	17	0.000616	0.020403
11 Endocytosis	255	12.674	25	0.000908	0.027319
12 FoxO signaling pathway	136	6.7593	16	0.001151	0.031744
13 Mitophagy - animal	65	3.2305	10	0.001285	0.03271
14 Chronic myeloid leukemia	77	3.8269	11	0.0014	0.0331
15 Human T-cell leukemia virus 1 infection	224	11.133	22	0.001764	0.038931

Figure 7. Comparison of metabolites between the PCOS patient data set and the ovary of BPA lineage fish. (A) A Venn diagram showing overlapped metabolites in both the PCOS patient data set and the ovary of BPA lineage fish. (B) Joint pathway analysis of transcriptome and metabolomes with list of the pathways with total hits, *P* value, and FDR.

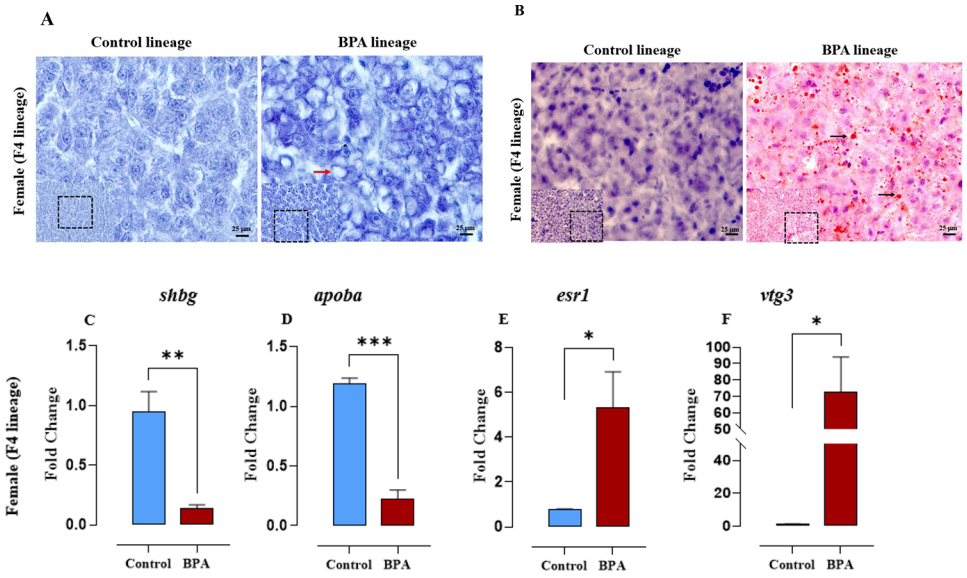

Figure 8. Ancestral BPA exposure resulted in liver steatosis in females of the F4 generation. (A) Liver histology micrograph. (B) Fat accumulation in the liver of the F4 generation females (magnification ×40). Transgenerational alterations in the expression of genes in BPA lineage livers. Significant decrease in (C) *shbg* and (D) *apoba* transcript in BPA lineage fish. Significant decrease in the levels of (E) *esr1* and (F) *vtg3* transcripts in BPA lineage fish. Asterisks indicate statistical significances at the level of $*P < 0.05$ and $***P < 0.001$ compared to control lineage by *t* test.

metabolic pathways associated with PCOS (Figure 6B). Biomarkers of PCOS were found in the ovary metabolite data. With $P < 0.05$ and AUC = 1, a total of 17 biomarkers were found in the ovary of the BPA lineage (Figure 6C). Those were inosine, guanosine, phosphocreatine, 2-methylcitric acid, taurodeoxycholic acid, 2,4-diamino-6-nitrotoluene, L-palmitoylcarnitine, xanthine, niacinamide, asymmetric dimethylarginine, all-*trans*-retinoic acid, hypoxanthine, nicotinic acid, ornithine, 6-(alpha-D-glucosaminyl)-1D-myo-inositol, glucosylceramide, and allysine (Figure S17). The top 25 highly enriched metabolic pathways were identified. Metabolically important pathways such as arginine biosynthesis, aminoacyl-tRNA biosynthesis, histidine metabolism, proline metabolism, and glutathione metabolism were highly enriched in the BPA lineage ovary (Figure S18).

3.4.1. Comparative Analysis of the Metabolites of BPA Lineage Fish Ovary with PCOS Patient Metabolite Data Set. To investigate potential metabolites linked to transgenerational PCOS, the metabolites of F4 ovary from BPA lineage were compared with the PCOS patient metabolite data.[81] A total of 16 metabolites were found to be common between BPA lineage and PCOS patients (Figure 7A). Among the 16 metabolites, 8 common metabolites showed a mutual pattern of abundance, and 7 of them showed an exclusive abundance pattern in the ovary of BPA lineage. Pregnenolone, eicosapentaenoic acid, phytosphingosine, azelaic acid, sphinganine, phenylpyruvic acid, ornithine, and inosine showed similar abundance patterns in the ovary of BPA lineage and PCOS patient data set (Figure 6A). However, creatinine, taurine, uridine, and taurine exhibited an exclusive pattern of abundance under common metabolites (Figure 6A). KEGG pathway analysis was conducted on common metabolites found in the ovary of BPA lineage and human patients. These pathways included sphingolipid metabolism, glutathione metabolism, phenylalanine, tyrosine and tryptophan metabolism, taurine metabolism, and hypotaurine metabolism (Figure S18).

3.4.2. Integrated Metabolomic and Transcriptomic Pathway Analysis Revealed Deleterious Pathways in the Ovary of BPA Lineage Fish. Significantly altered metabolites and

https://doi.org/10.1021/acs.est.3c01922
Environ. Sci. Technol. 2023, 57, 12602−12619

genes were submitted to joint pathway analysis in Metaboanalyst.[84] Out of the 324 biological processes identified, 74 pathways had P value < 0.05 and FDR < 25%. The top three pathways based on the calculation of P value were the ABC transporter, carbon metabolism in cancer, and arginine biosynthesis (Figure 7B). The gene−metabolite interaction network and metabolite−metabolite interaction network are shown in Figure S19. Metabolites found in carbon metabolism for triggering cancer were mapped in Figure S20. The insulin signaling, endocytosis, and cancer-related pathways that were found prominent in both omics were also significantly enriched in the integrative analysis.

3.5. Abnormal Fat Accumulation and Hepatosteatosis in the Liver of the F4 Females. The liver in the BPA lineage females had more vacuolated hepatocytes than in the control lineage fish (Figure 8A). The hepatic cells were arranged in sheets separated by sinusoidal meshes. To determine if ancestral BPA exposure caused lipid accumulation in the liver, which is also a symptom of NAFLD, Oil Red O was used to stain hepatic neutral lipids. Consistent with their higher hepatosomatic index (HSI), cryosections of the livers of the BPA lineage females showed a proportional accumulation of neutral lipids (Figure 8B), indicating the liver of BPA lineage developing NAFLD.

3.6. Expression of Vitellogenic and Sex Hormone Binding Globulin Genes in the Liver. To examine whether ancestral BPA exposure altered the expression of vitellogenic genes in the F4 generation liver, expression profiles of the vitellogenic genes were determined by qPCR. The mRNA levels of the sex hormone binding globulin (*shbg*) gene, a PCOS marker,[85] were significantly decreased in the BPA lineage livers (Figure 8C). Furthermore, the expression of genes involved in vitellogenin synthesis pathway in the liver was significantly altered. Mainly, the expression of apolipoprotein ba (*apoba*) was significantly downregulated (Figure 8D), and both estrogen receptor 1 (*esr1*) and vitellogenin 3 (*vtg3*) were significantly upregulated (Figure 8E,F) in the BPA lineage.

4. DISCUSSION

According to familial clustering and twin studies, PCOS is an inherited disease.[86,87] Given that approximately 10% of its human PCOS loci are genetic and inherited,[88] the overall pathogenesis of PCOS suggests its onset and regulation by environmental and nongenetic mechanisms. Environmental chemical exposures during germ cell reprogramming can leave chemical-specific epigenetic marks on germ cells, which result in phenotypic abnormalities that persist through several generations.[89−91] When directly exposed to BPA, females develop metabolic disorders or PCOS in the immediate generation (F0).[92−95] However, it is not clearly understood whether future-generation females can still suffer metabolic and reproductive diseases even after the withdrawal of BPA from consumer products and the environment. This study demonstrates for the first time using medaka fish as an animal model that embryonic exposure to BPA during germ cell reprogramming in a grandparental generation leads to multidisease transgenerational phenotypes, PCOS, and NAFLD in the fifth generation who did not experience BPA exposure. The hypothalamus−pituitary−gonad (HPG) axis in fish resembles that in mammals, suggesting a great potential to study human PCOS as an alternative nonmammalian model.[36,37,40] Medaka and zebrafish utilize similar pathways of sex hormonal regulation of steroidogenesis but process epigenome in their embryo and germline cells differently.[39] Unlike other fish species, medaka processes epigenetic information in postfertilization embryos and primordial germ cells similar to humans and mice, making them excellent transgenerational models.[38,39] This suggests that the mechanistic molecular information obtained from medaka could be valuable for understanding ancestral epigenetic effects of BPA in the development of PCOS in the subsequent generation of other higher vertebrates, including humans.

In the present study, F4 females of the BPA lineage group displayed abnormal metabolic traits, such as increased BMI and visceral fat accumulation. The ability of BPA to induce fat accumulation has been demonstrated in a direct exposure model. BPA caused insulin resistance and disrupted lipid homeostasis in primary human preadipocytes, resulting in abnormal fat accumulation *in vitro*,[96−100] suggesting BPA's ability to modulate fat deposition due to chronic exposure. However, how visceral fat deposition occurs in unexposed generations due to ancestral exposure is unclear. In addition to transgenerational fat deposition in the BPA lineage group, significant upregulation of the expression of *il6* and genes encoding several cytokines and downregulation of *igf1* were found in the ovary of the BPA lineage, indicating a potential state of insulin resistance mediated by visceral fat accumulation. Congruent with a previous study, an altered expression pattern, particularly the upregulation of *il6* and activation of *tnf-α*, a master regulator, was found in the ovary of BPA lineage, indicating visceral fat mediation due to the activation of proinflammatory cytokines (*TNF-α*, *IL-6*) and tissue macrophages, critical drivers of PCOS-obesity multifactorial disease.[101,102] The downregulation of *igf1* in the ovary of the BPA lineage could also have contributed to impaired follicular growth, as reflected histologically. The literature shows decreased levels of IGF-I and IGF-II proteins in the follicular fluid of PCOS women as well as reduced expression of IGF-1 receptor in human granulosa cells,[103,104] suggesting the role of IGF protein in PCOS development. The present observations provide an additional line of information that environmentally induced transgenerational fat deposition could have activated cytokines and decreased follicular maturation in females of the BPA lineage, leading to PCOS phenotype.

The gonadotropins play a vital role in PCOS pathogenesis, and in the teleost, they regulate the vitellogenesis and final oocyte maturation/ovulation.[105,106] In the present study, lower levels of *fshr* mRNA and higher levels of *lhr* mRNA were detected in the ovary of BPA lineage fish than in the control. In teleost, gonadotropin receptor expression positively correlates with plasma hormone levels.[107] The present results indicated lower levels of mRNAs for FSH and higher levels of LH in the ovary of BPA lineage fish, suggesting transgenerational hormonal imbalance. A high LH/FSH ratio is a characteristic of PCOS patients. Similar patterns of gonadotropin receptor gene expression suggest a similar trend.[108] Increased levels of plasma FSH and ovarian follicle-stimulating hormone receptor (*FSHr*) mRNA levels are required for the transition of oocytes from the previtellogenic stage (stage II) to vitellogenic stages (stage III) during ovarian maturation.[106,109,110] In the present study, abnormal follicular development in stage II (previtellogenic oocyte) was found, along with the downregulation of *fshr* in the ovary of BPA lineage. Ovarian follicles are arrested at the primary growth-previtellogenic transition in zebrafish mutant for *fshr*.[111] The restricted maturation of follicles observed in

https://doi.org/10.1021/acs.est.3c01922
Environ. Sci. Technol. 2023, 57, 12602−12619

the ovary of BPA lineage medaka that leads to anovulation could be due to deficiency of *fshr*, which is a primary phenotype for PCOS.[112] Consistent with our present histopathological findings in medaka, similar histological phenotypes were found in the rat model of PCOS, suggesting that the BPA lineage group had developed PCOS phenotype in the ovary.[113] Direct exposure to BPA has been linked to follicular arrest and atresia leading to anovulation,[114−116] suggesting that transgenerational PCOS could be driven by mechanisms similar to those reported from direct exposure studies. The critical yet undiscovered information is delineating heritable molecular determinants of PCOS and developing strategies to block pathways to disease, as environmental BPA exposure (past and present) might already have left such molecular memories in the germline of the existing population.

The development of PCOS is intrinsically linked to steroidogenic dysregulation. The upregulation of androgenic genes such as *3β-hsd*, *hsd17b1*, and *cyp11a* in the ovary of BPA lineage medaka could have potentially enhanced testosterone biosynthesis in ovarian theca cells. This can be validated by a human study in which a positive association of increased free testosterone (hyperandrogenemia) was found with increased visceral fat deposits in women with PCOS.[117] This clearly suggests that transgenerational deposition of visceral fat could be due to the biosynthesis of testosterone in BPA lineage females. In contrast, the expression of *Cyp19a1a*, the gene encoding estrogen-synthesizing enzyme aromatase, was increased in the ovary of the BPA lineage females. The fold change of androgenic genes was more significant than that of estrogen-synthesizing genes, indicating an increase in the hypothetical ratio of androgen/estrogen, a characteristic of PCOS.[118] An *in vitro* study found that hyperactivation of *lhr* increases adenylate cyclase, which triggers the synthesis of *3β-hsd*.[119,120] Increased levels of LH boost the synthesis of androgen from theca cells of the ovary leading to ovarian dysfunction.[121,122] Congruent with our observation, the upregulation of *lhr* expression could have induced the upregulation of *3β-hsd*, enhancing androgen synthesis in the ovary. As a result, dysregulation of the steroidogenic pathway could have contributed to potential reproductive impairment related to the PCOS phenotype in the F4 BPA lineage fish.

PCOS-specific DEGs activated in the ovary of BPA lineage fish were compared with the PCOS patient transcriptome data set. In total, 292 common significant DEGs were determined, potentially contributing to pathogenesis, including genes associated with activating the TNF signaling pathway, endocrine resistance, and cancer pathway. Consistent with GSEA analysis, IPA revealed canonical pathways such as autophagic mechanism, cell cycle regulation, cellular stress and injury, and cancer pathway with the activation of AKT1 and TNF. Interestingly, genes associated with activating the cancerous pathway, i.e., *myc*, *akt1*, *apc*, and *mtor*, were upregulated in the ovary of the BPA lineage group. Alternatively, the ovary of the BPA lineage group showed decreased expression of *foxo1* and tumor suppressor gene (*smad 4*) genes. Upregulation of c-MYC, enhanced AKT activity, activated protein C (APC), and reduced FOXO3a activity were observed in epithelial ovarian carcinoma.[123−126] In line with a previous study conducted by Bornstein *et al.* showing that a loss in SMAD4 increases genomic instability associated with the TGF-*β* signaling in ovarian cancer, increased expression of *tgf-β* in the ovary of BPA lineage was detected, suggesting an advanced stage of ovarian disease.[127] Among the top 10 upregulated genes, three genes, namely, *selenop*, *RNA-nf1*, and *olfml3*, were associated with sex-hormone modulation[128] and found in PCOS follicular fluid,[129] controlling cell cycle progression associated with ovarian teratoma.[130] In the top 10 downregulated genes, *fabp6* and *arl6* (ADP ribosylation factor like GTPase6) were involved in ovarian disease[131] and modulating membrane trafficking and cytoskeletal function.[132] As transcriptional dysregulation and diseases are influenced by chromatin organization,[133] we were interested in deciphering epigenetic gene expression controlling the transcriptional output of the cell. Among the 91 DEGs found to be involved in chromatin organization, *kdm2b*, *ehmt1*, *hdac4*, *kmt2d*, *jmjd6*, *ctcf*, *setd5*, *suz12*, *btaf1*, and *bahd1* were all upregulated, whereas *dnmt3ba* and *dnmt3b* were downregulated, indicating transgenerational alteration of epigenetic genes associated with PCOS phenotype in the ovary of BPA lineage. Previous studies showed that upregulation of KDM2B and HDAC and dysregulation of EHMT1/2 are linked to DNA damage and dysregulation of the cell cycle, and overexpression of *HDAC* is linked to ovarian cancer.[134,135] Together with the published literature, differential expression of PCOS-specific genes and epigenetic genes linked to histone modifications and DNA methylation indicates a role of epigenetic genes associated with PCOS phenotype in the ovary of BPA lineage fish.

In the ovary of the BPA lineage fish, several transforming growth factors (TGFs) were differentially expressed, indicating activation of several downstream genes such as fibrotic genes such as *col1a1b*, *cola2*, *col2a1a*, *jun*, *foxo3*, *sp1*, and *olfml3* and extracellular matrix protein genes. In addition, the expressions of *hspa5* and *eif2ak3* (unfolded protein response (UPR) genes) were upregulated in the BPA lineage ovary compared to control, indicating that ER stress response could have potentially activated the TGF *β* pathway.[136] The ovary of the BPA lineage fish showed significant upregulation of several transforming growth factors, including upstream regulators *tgfb1* and *tgfb3*, indicating the activation of several downstream fibrotic genes such as *col1a1b*, *cola2*, *col2a1a*, *jun*, *foxo3*, and *sp1*. The ovary of the BPA lineage fish also showed extracellular tissue deposition in accordance with the activation of fibrotic genes and extracellular matrix protein gene *olfml3*. Expression of genes related to ER stress, UPR, and TGF-1 was upregulated in granulosa cells of the ovary and was linked to tissue fibrosis.[137−140] Extracellular matrix accumulation in the form of collagen deposition in the ovarian capsule of the BPA lineage is linked to PCOS pathogenesis.[141] Using GSEA analysis, 94 DEGS were identified as associated with autophagy, including upregulated *atg3*, *becn2*, and *casp3* and downregulated foxo1 genes, suggesting aberrant autophagic mechanism activated in the ovary of the BPA lineage. The literature suggests that ATG3 and Foxo1 levels are downregulated in PCOS patients and that decreased levels of autophagy markers (ATG7 and BECN1) directly inhibit oocyte maturation.[142,143] Moreover, an elevated *caspase3* expression in the ovary, which is a biomarker for PCOS, can trigger aberrant apoptosis resulting in the development of cysts resulting from degenerated follicles found in the ovary of the BPA lineage.[144] Direct exposure to BPA has been found to activate proinflammatory cytokines IL6 and TNF*α* that are involved in fibrosis.[145] However, in transgenerational PCOS ovaries, activation of the TGF signaling pathway and ER stress response was synergistically involved in fibrosis induced by ancestral BPA exposure.

https://doi.org/10.1021/acs.est.3c01922
Environ. Sci. Technol. 2023, 57, 12602−12619

Compared with the previous metabolomic studies on follicular fluid from PCOS patients, the changes in several metabolites in the ovary of BPA lineage were consistent with PCOS patients.[81] Mutual metabolites were significantly enriched in sphingolipid metabolism, glutathione metabolism, taurine, hypotaurine metabolism, and phenylalanine metabolism. An abnormal expression of sphingolipids such as lysophosphatidylcholines and phosphatidylethanolamines was found to be associated with PCOS.[82] Physiological deviations in amino acid concentrations may lead to pathogenic conditions, such as oxidative stress and ovarian disease, as well as metabolic disturbances, such as type 2 diabetes, obesity, and insulin resistance.[146−148] A high abundance of valine, histidine, tryptophan, and creatinine was found in the BPA lineage group. In agreement with our finding, an analysis performed by Zhao *et al.* found that the levels of alanine, valine, serine, threonine, ornithine, phenylalanine, tyrosine, and tryptophan are generally increased and the levels of glycine and proline are reduced in plasma samples of PCOS patients.[82] In the present study, PCOS-specific pathways, including arginine biosynthesis,[149,150] aminoacyl-tRNA biosynthesis,[151,152] beta-alanine metabolism,[150] proline and arginine metabolism,[153,154] taurine metabolism,[155] and phenylalanine metabolism,[150] were activated in the ovary of the BPA lineage group, suggesting that metabolic alterations were promoted by ancestral BPA exposure effect.

The present results from a human−fish comparative metabolomics−transcriptome analysis show distinctly altered ABC transporter, central carbon metabolism in cancer, aminoacyl-tRNA biosynthesis, protein digestion, and absorption pathways, indicating that BPA has a potential role in the development of PCOS in fish and humans. Changes in the ATP binding cassette transporter 1 (ABC1) gene, which encodes the protein regulating entry and exit from the cell membrane, may contribute to dyslipidemia in patients with PCOS.[156,157] In addition, the top five significantly enriched KEGG pathways for PCOS vs premature ovarian follicle (POF) group metabolites included protein digestion and absorption pathways, ABC transporter-dependent pathways, central carbon metabolism pathways in cancer, aminoacyl-tRNA biosynthesis pathway, and prostate cancer pathways found in human studies.[158] Additionally, arginine proline metabolism, insulin signaling pathway, and lysosomal pathways were found to be involved in ancestral BPA exposure-induced PCOS. A KEGG pathway analysis indicated that insulin signaling, MAPK signaling, AMPK signaling pathway, and autophagic pathway were enriched by total upregulated genes, whereas Rap1, cAMP, and AGE-RAGE signaling pathways were enriched by total downregulated genes, indicating PCOS-specific pathways in the ovary of the BPA lineage. Activation of the Rap1 signaling pathway is found in cancer, and AGE-RAGE signaling is involved in the pathogenesis of diabetes.[159,160] Several studies have shown that PCOS is associated with impaired insulin signaling, aberrant MAPK signaling, and abnormal AMPK signaling in ovarian cumulus and granulosa cells.[66,161,162] The present results, together with the published literature on PCOS development and progression, show that ancestral BPA exposure seems to have activated deleterious signaling pathways in the ovary of the BPA lineage leading to advanced-stage ovarian disease. The PCOS phenotype was observed in females that developed severe NALFD.

The presence of low *apoB* transcript in the liver of BPA lineage females was accompanied by significant fat accumulation, suggesting that a lack of fat molecules released by the liver may have contributed to abnormal fat accumulation, as indicated by the oil and red stain in the liver. Downregulation of *apoB* isoforms may result in low levels of TGs and cholesterol in the circulation as well as an extensive accumulation of lipid droplets in hepatocytes, indicating the development of NAFLD phenotype.[163] In BPA lineage females, the levels of *shbg* mRNAs were significantly decreased in the liver, suggesting another possible link between transgenerational PCOS and NAFLD. The PCOS biomarker SHBG protein is a circulating homodimeric glycoprotein synthesized by hepatocytes with a stronger affinity for testosterone than estrogen.[164] The expression of *shbg* was decreased in the liver of the BPA lineage females. Such a decrease in expression has been found to positively correlate with the bioavailability of free testosterone,[165] hyperandrogenism,[166] fatty liver disease, hyperinsulinemia, and PCOS. These observations reflect a cross talk between the hepato-ovarian axis in BPA lineage fish. Additionally, the F4 generation of the BPA lineage group showed highly upregulated *esr1* and *vtg3* transcripts in the liver, indicating estrogen-mediated induction of vitellogenin synthesis that enhances fat body synthesis in the liver.[167] However, the uptake of vitellogenin via the vitellogenin receptor in the ovary is highly important for the maturation of oocytes in teleost to maintain a steady state of follicular balance.[168] In the BPA lineage fish, vitellogenin receptor (*vtgr*) expression was significantly reduced, suggesting a perturbed vitellogenin uptake that could have prevented the transition from previtellogenic to vitellogenic oocytes and promoted the immature follicular state related to the PCOS phenotype in the BPA lineage fish.

The present results demonstrate a multidisease phenotype of NAFLD−PCOS in females four generations after direct embryonic BPA exposure at F0 generation. At this time of embryonic development, the liver and gonadal germline cells are differentiating from their progenitor cells. Results suggest that BPA exposure not only causes PCOS in an immediate generation but also can cause multidisease phenotype in offspring after several generations, via germline transmission. Integration of both transcriptomic and metabolomic results revealed the presence of affected metabolic routes in the ovary of the BPA lineage, suggesting a potential mechanism underlying transgenerational reproductive impairment. Together with the transgenerational inheritance concept of the published literature, the present study suggests that ancestral BPA exposure-induced molecular memories, not yet discovered, may be promoting these multidisease phenotypes. Environmentally established molecular memories are transferred from the germline to the somatic cells (e.g., liver and ovary).[7] To demonstrate causative relationships between germline epigenome and observed transgenerational phenotypic traits in the ovary and liver, it is imperative to screen the ancestral germline epimutations induced by BPA and correlate them with epigenomes of liver and ovary of subsequent generations and their manipulation by CRISPR-mediated epigenome editing to understand their role in the development of multidisease phenotypes.

https://doi.org/10.1021/acs.est.3c01922
Environ. Sci. Technol. 2023, 57, 12602−12619

■ ASSOCIATED CONTENT

Supporting Information

The Supporting Information is available free of charge at https://pubs.acs.org/doi/10.1021/acs.est.3c01922.

A global alteration in gene expression in the ovary of the BPA lineage exhibited by heatmap (Figure S1); Gene Ontology analysis in the ovary of BPA lineage (Figure S2); DEGs enriched in the insulin signaling pathway in the ovary of BPA lineage (Figure S3); DEGs found in the MAPK signaling pathway in the ovary of BPA lineage (Figure S4); DEGs enriched in the AMPK signaling pathway in the ovary of BPA lineage (Figure S5); DEGs found in the Rap1 signaling pathway in the ovary of BPA lineage (Figure S6); DEGs found in the cAMP signaling pathway in the ovary of BPA lineage (Figure S7); standard GSEA analysis and heatmap of enriched DEGs associated with pathogenesis (Figures S8 and S9); the PCOS-specific mutual DEGs in the ovary of the BPA lineage fish and PCOS patient data set (Figure S10); molecular mechanism of the cancer triggering pathway in the ovary of the BPA lineage fish (Figure S11); molecular mechanism of the autophagy triggering pathway in the ovary of the BPA lineage fish (Figure S12); molecular mechanism of the HOTAIR mechanism in the ovary of the BPA lineage fish (Figure S13); gene disease network via Ingenuity Pathway Analysis (IPA) showing activation of *akt1*, *tnf*, and *ifng* associated with activation of disease specific pathways (Figure S14); predicted top 15 upstream regulator determined by IPA (Figure S15); score plot showing significant difference in metabolites (Figure S16); categorization of significant metabolites (VIP > 1) found in the ovary of the BPA lineage (Figure S17); the enrichment of metabolites is associated with several metabolic pathways (Figure S18); gene metabolite interaction network in the ovary of BPA lineage showing positive association of metabolites with gene expression (Figure S19); and mapping of differential metabolites and genes found in the carbon metabolism of cancer (Figure S20) (PDF)

■ AUTHOR INFORMATION

Corresponding Author

Ramji Kumar Bhandari − *Department of Biology, University of North Carolina at Greensboro, Greensboro 27412 North Carolina, United States;* orcid.org/0000-0001-5608-7254; Email: rkbhanda@uncg.edu

Authors

Sourav Chakraborty − *Department of Biology, University of North Carolina at Greensboro, Greensboro 27412 North Carolina, United States*

Santosh Anand − *Department of Biology, University of North Carolina at Greensboro, Greensboro 27412 North Carolina, United States*

Seraiah Coe − *Department of Biology, University of North Carolina at Greensboro, Greensboro 27412 North Carolina, United States*

Beh Reh − *Department of Biology, University of North Carolina at Greensboro, Greensboro 27412 North Carolina, United States*

Complete contact information is available at: https://pubs.acs.org/10.1021/acs.est.3c01922

Author Contributions

R.K.B. conceptualized and supervised the research. S.C., R.K.B., S.T.C., and B.R. performed experiments. S.A. performed bioinformatic data analysis. B.R. is an undergraduate student.

Notes

The authors declare no competing financial interest.

■ ACKNOWLEDGMENTS

This study was supported by funds from the National Institutes of Health (R01ES032452, R21ES027123, and R21HD098621) to R.K.B. and the University of North Carolina at Greensboro Graduate School to S.C. The authors thank Pooja Bhandari (Research Technician) and undergraduate researchers (Triquina Harrison, Donajah Cherry, and Tyler Niles) for their assistance in animal care.

■ REFERENCES

(1) Shi, M.; Whorton, A. E.; Sekulovski, N.; MacLean, J. A., II; Hayashi, K. Prenatal Exposure to Bisphenol A, E, and S Induces Transgenerational Effects on Male Reproductive Functions in Mice. *Toxicol. Sci.* **2019**, *172*, 303−315.

(2) Mao, Z.; Xia, W.; Chang, H.; Huo, W.; Li, Y.; Xu, S. Paternal BPA exposure in early life alters Igf2 epigenetic status in sperm and induces pancreatic impairment in rat offspring. *Toxicol. Lett.* **2015**, *238*, 30−38.

(3) Zhu, L.; Yuan, C.; Wang, M.; Liu, Y.; Wang, Z.; Seif, M. M. J. A. Bisphenol A-associated alterations in DNA and histone methylation affects semen quality in rare minnow *Gobiocypris rarus*. *Aquat. Toxicol.* **2020**, *226*, No. 105580.

(4) Drobná, Z.; Henriksen, A. D.; Wolstenholme, J. T.; Montiel, C.; Lambeth, P. S.; Shang, S.; Harris, E. P.; Zhou, C.; Flaws, J. A.; Adli, M.; Rissman, E. F. Transgenerational Effects of Bisphenol A on Gene Expression and DNA Methylation of Imprinted Genes in Brain. *Endocrinology* **2018**, *159*, 132−144.

(5) Manikkam, M.; Tracey, R.; Guerrero-Bosagna, C.; Skinner, M. K. Plastics derived endocrine disruptors (BPA, DEHP and DBP) induce epigenetic transgenerational inheritance of obesity, reproductive disease and sperm epimutations. *PLoS One* **2013**, *8*, No. e55387.

(6) Salian, S.; Doshi, T.; Vanage, G. Perinatal exposure of rats to Bisphenol A affects the fertility of male offspring. *Life Sci.* **2009**, *85*, 742−752.

(7) Rahman, M. S.; Pang, W. K.; Ryu, D. Y.; Park, Y. J.; Pang, M. G. Multigenerational and transgenerational impact of paternal bisphenol A exposure on male fertility in a mouse model. *Hum. Reprod.* **2020**, *35*, 1740−1752.

(8) Wang, X.; Hill, D.; Tillitt, D. E.; Bhandari, R. K. Bisphenol A and 17alpha-ethinylestradiol-induced transgenerational differences in expression of osmoregulatory genes in the gill of medaka (*Oryzias latipes*). *Aquat. Toxicol.* **2019**, *211*, 227−234.

(9) Lombó, M.; Fernández-Díez, C.; González-Rojo, S.; Navarro, C.; Robles, V.; Herráez, M. P. Transgenerational inheritance of heart disorders caused by paternal bisphenol A exposure. *Environ. Pollut.* **2015**, *206*, 667−678.

(10) Wolstenholme, J. T.; Goldsby, J. A.; Rissman, E. F. Transgenerational effects of prenatal bisphenol A on social recognition. *Horm. Behav.* **2013**, *64*, 833−839.

(11) Wolstenholme, J. T.; Edwards, M.; Shetty, S. R. J.; Gatewood, J. D.; Taylor, J. A.; Rissman, E. F.; Connelly, J. J. Gestational exposure to bisphenol a produces transgenerational changes in behaviors and gene expression. *Endocrinology* **2012**, *153*, 3828−3838.

(12) Dabeer, S.; Afjal, M.; Ahmad, S.; Fatima, M.; Habib, H.; Parvez, S.; Raisuddin, S. Transgenerational effect of parental obesity and chronic parental bisphenol A exposure on hormonal profile and

reproductive organs of preadolescent Wistar rats of F1 generation: A one-generation study. *Hum. Exp. Toxicol.* **2020**, *39*, 59−76.
(13) Frankowski, R.; Zgoła-Grześkowiak, A.; Grześkowiak, T.; Sójka, K. The presence of bisphenol A in the thermal paper in the face of changing European regulations−A comparative global research. *Environ. Pollut.* **2020**, *265*, No. 114879.
(14) Møller, L.; Fotel, F.; Larsen, P. Survey of bisphenol A and bisphenol-A diglycidylether polymer. *The Danish Environmental Protection Agency*.2013/04 https://www2.mst.dk/udgiv/publications/2013/04/978-87-93026-14-8.pdf. 2013 ().
(15) Cwiek-Ludwicka, K. Bisphenol A (BPA) in food contact materials-new scientific opinion from EFSA regarding public health risk. *Rocz. Panstw. Zakl. Hig.* **2015**, *66* ().
(16) Chakraborty, S.; Dissanayake, M.; Godwin, J.; Wang, X.; Bhandari, R. K. Ancestral BPA exposure caused defects in the liver of medaka for four generations. *Sci. Total Environ.* **2023**, *856*, No. 159067.
(17) Albertini, D.; Combelles, C.; Benecchi, E.; Carabatsos, M. Cellular basis for paracrine regulation of ovarian follicle development. *Reproduction* **2001**, *121*, 647−653.
(18) Gilchrist, R. B.; Ritter, L. J.; Armstrong, D. T. Oocyte−somatic cell interactions during follicle development in mammals. *Anim. Reprod. Sci.* **2004**, *82-83*, 431−446.
(19) Sudhakaran, G.; Guru, A.; Muthu, B. H. D.; Murugan, R.; Arshad, A.; Arockiaraj, J. Evidence-based hormonal, mutational, and endocrine-disrupting chemical-induced zebrafish as an alternative model to study PCOS condition similar to mammalian PCOS model. *Life Sci.* **2022**, *291*, No. 120276.
(20) Lerchbaum, E.; Schwetz, V.; Rabe, T.; Giuliani, A.; Obermayer-Pietsch, B. Hyperandrogenemia in polycystic ovary syndrome: exploration of the role of free testosterone and androstenedione in metabolic phenotype. *PLoS One* **2014**, *9*, No. e108263.
(21) Homburg, R. Management of infertility and prevention of ovarian hyperstimulation in women with polycystic ovary syndrome. *Best Pract. Res., Clin. Obstet. Gynaecol.* **2004**, *18*, 773−788.
(22) Pivonello, C.; Muscogiuri, G.; Nardone, A.; Garifalos, F.; Provvisiero, D. P.; Verde, N.; de Angelis, C.; Conforti, A.; Piscopo, M.; Auriemma, R. S.; Colao, A.; Pivonello, R. Bisphenol A: an emerging threat to female fertility. *Reprod. Biol. Endocrinol.* **2020**, *18*, 22.
(23) Tran, D. N.; Jung, E.-M.; Ahn, C.; Lee, J.-H.; Yoo, Y.-M.; Jeung, E.-B. Effects of bisphenol A and 4-tert-octylphenol on embryo implantation failure in mouse. *Int. J. Environ. Res. Public Health* **2018**, *15*, 1614.
(24) Aloisi, A. M.; Della Seta, D.; Ceccarelli, I.; Farabollini, F. Bisphenol-A differently affects estrogen receptors-α in estrous-cycling and lactating female rats. *Neurosci. Lett.* **2001**, *310*, 49−52.
(25) Li, Y.; Zhang, W.; Liu, J.; Wang, W.; Li, H.; Zhu, J.; Weng, S.; Xiao, S.; Wu, T. Prepubertal bisphenol A exposure interferes with ovarian follicle development and its relevant gene expression. *Reprod. Toxicol.* **2014**, *44*, 33−40.
(26) Singh, S.; Li, S. S.-L. Epigenetic effects of environmental chemicals bisphenol A and phthalates. *Int. J. Mol. Sci.* **2012**, *13*, 10143−10153.
(27) Lombó, M.; Fernández-Díez, C.; González-Rojo, S.; Herráez, M. P. Genetic and epigenetic alterations induced by bisphenol A exposure during different periods of spermatogenesis: from spermatozoa to the progeny. *Sci. Rep.* **2019**, *9*, 18029.
(28) Zheng, H.; Zhou, X.; Li, D. K.; Yang, F.; Pan, H.; Li, T.; Miao, M.; Li, R.; Yuan, W. Genome-wide alteration in DNA hydroxymethylation in the sperm from bisphenol A-exposed men. *PLoS One* **2017**, *12*, No. e0178535.
(29) Targher, G.; Rossini, M.; Lonardo, A. Evidence that non-alcoholic fatty liver disease and polycystic ovary syndrome are associated by necessity rather than chance: a novel hepato-ovarian axis? *Endocrine* **2016**, *51*, 211−221.
(30) Chauvin, S.; Cohen-Tannoudji, J.; Guigon, C. J. Estradiol Signaling at the Heart of Folliculogenesis: Its Potential Deregulation in Human Ovarian Pathologies. *Int. J. Mol. Sci.* **2022**, *23*, 512.
(31) Kandaraki, E.; Chatzigeorgiou, A.; Livadas, S.; Palioura, E.; Economou, F.; Koutsilieris, M.; Palimeri, S.; Panidis, D.; Diamanti-Kandarakis, E. Endocrine disruptors and polycystic ovary syndrome (PCOS): elevated serum levels of bisphenol A in women with PCOS. *J. Clin. Endocrinol. Metab.* **2011**, *96*, E480−E484.
(32) Hu, Y.; Wen, S.; Yuan, D.; Peng, L.; Zeng, R.; Yang, Z.; Liu, Q.; Xu, L.; Kang, D. The association between the environmental endocrine disruptor bisphenol A and polycystic ovary syndrome: a systematic review and meta-analysis. *Gynecol. Endocrinol.* **2018**, *34*, 370−377.
(33) Brzozowska, M. M.; Ostapowicz, G.; Weltman, M. D. An association between non-alcoholic fatty liver disease and polycystic ovarian syndrome. *J. Gastroenterol. Hepatol.* **2009**, *24*, 243−247.
(34) Markou, A.; Androulakis, I. I.; Mourmouris, C.; Tsikkini, A.; Samara, C.; Sougioultzis, S.; Piaditis, G.; Kaltsas, G. Hepatic steatosis in young lean insulin resistant women with polycystic ovary syndrome. *Fertil. Steril.* **2010**, *93*, 1220−1226.
(35) Hossain, N.; Stepanova, M.; Afendy, A.; Nader, F.; Younossi, Y.; Rafiq, N.; Goodman, Z.; Younossi, Z. M. Non-alcoholic steatohepatitis (NASH) in patients with polycystic ovarian syndrome (PCOS). *Scand. J. Gastroenterol.* **2011**, *46*, 479−484.
(36) Lessman, C. A. Oocyte maturation: converting the zebrafish oocyte to the fertilizable egg. *Gen. Comp. Endocrinol.* **2009**, *161*, 53−57.
(37) Rosenfield, R. L.; Ehrmann, D. A. The pathogenesis of polycystic ovary syndrome (PCOS): the hypothesis of PCOS as functional ovarian hyperandrogenism revisited. *Endocr. Rev.* **2016**, *37*, 467−520.
(38) Naruse, K.; Tanaka, M.; Takeda, H. *Medaka: a model for organogenesis, human disease, and evolution*. Springer Science & Business Media: 2011, DOI: 10.1007/978-4-431-92691-7.
(39) Wang, X.; Bhandari, R. K. DNA methylation reprogramming in medaka fish, a promising animal model for environmental epigenetics research. *Environ. Epigenet.* **2020**, *6*, No. dvaa008.
(40) Hoo, J. Y.; Kumari, Y.; Shaikh, M. F.; Hue, S. M.; Goh, B. H. Zebrafish: A Versatile Animal Model for Fertility Research. *BioMed Res. Int.* **2016**, *2016*, No. 9732780.
(41) Wang, X.; Bhandari, R. K. The dynamics of DNA methylation during epigenetic reprogramming of primordial germ cells in medaka (Oryzias latipes). *Epigenetics* **2020**, *15*, 483−498.
(42) Tanaka, M.; Kinoshita, M.; Kobayashi, D.; Nagahama, Y. Establishment of medaka (Oryzias latipes) transgenic lines with the expression of green fluorescent protein fluorescence exclusively in germ cells: a useful model to monitor germ cells in a live vertebrate. *Proc. Natl. Acad. Sci.* **2001**, *98*, 2544−2549.
(43) Ryan, K. K.; Haller, A. M.; Sorrell, J. E.; Woods, S. C.; Jandacek, R. J.; Seeley, R. J. Perinatal exposure to bisphenol-a and the development of metabolic syndrome in CD-1 mice. *Endocrinology* **2010**, *151*, 2603−2612.
(44) Angle, B. M.; Do, R. P.; Ponzi, D.; Stahlhut, R. W.; Drury, B. E.; Nagel, S. C.; Welshons, W. V.; Besch-Williford, C. L.; Palanza, P.; Parmigiani, S.; vom Saal, F. S.; Taylor, J. A. Metabolic disruption in male mice due to fetal exposure to low but not high doses of bisphenol A (BPA): evidence for effects on body weight, food intake, adipocytes, leptin, adiponectin, insulin and glucose regulation. *Reprod. Toxicol.* **2013**, *42*, 256−268.
(45) Puttabyatappa, M.; Martin, J. D.; Andriessen, V.; Stevenson, M.; Zeng, L.; Pennathur, S.; Padmanabhan, V. Developmental programming: Changes in mediators of insulin sensitivity in prenatal bisphenol A-treated female sheep. *Reprod. Toxicol.* **2019**, *85*, 110−122.
(46) Marmugi, A.; Ducheix, S.; Lasserre, F.; Polizzi, A.; Paris, A.; Priymenko, N.; Bertrand-Michel, J.; Pineau, T.; Guillou, H.; Martin, P. G.; Mselli-Lakhal, L. Low doses of bisphenol A induce gene expression related to lipid synthesis and trigger triglyceride accumulation in adult mouse liver. *Hepatology* **2012**, *55*, 395−407.
(47) Samardzija, D.; Pogrmic-Majkic, K.; Fa, S.; Stanic, B.; Jasnic, J.; Andric, N. Bisphenol A decreases progesterone synthesis by

disrupting cholesterol homeostasis in rat granulosa cells. *Mol. Cell. Endocrinol.* **2018**, *461*, 55−63.
(48) Thayil, A. J.; Wang, X.; Bhandari, P.; vom Saal, F. S.; Tillitt, D. E.; Bhandari, R. K. Bisphenol A and 17α-ethinylestradiol-induced transgenerational gene expression differences in the brain−pituitary−testis axis of medaka, Oryzias latipes†. *Biol. Reprod.* **2020**, *103*, 1324−1335.
(49) Bhandari, R. K.; vom Saal, F. S.; Tillitt, D. E. Transgenerational effects from early developmental exposures to bisphenol A or 17α-ethinylestradiol in medaka, Oryzias latipes. *Sci. Rep.* **2015**, *5*, 9303.
(50) Iwamatsu, T. Stages of normal development in the medaka Oryzias latipes. *Mech. Dev.* **2004**, *121*, 605−618.
(51) Bhandari, R. K.; vom Saal, F. S.; Tillitt, D. E. Transgenerational effects from early developmental exposures to bisphenol A or 17alpha-ethinylestradiol in medaka, Oryzias latipes. *Sci. Rep.* **2015**, *5*, 9303.
(52) Hattori, R. S.; Gould, R. J.; Fujioka, T.; Saito, T.; Kurita, J.; Strussmann, C. A.; Yokota, M.; Watanabe, S. Temperature-dependent sex determination in Hd-rR medaka *Oryzias latipes*: gender sensitivity, thermal threshold, critical period, and *DMRT1* expression profile. *Sex. Dev.* **2007**, *1*, 138−146.
(53) Smith, C. M.; Vera, M. K. M.; Bhandari, R. K. Developmental and epigenetic effects of Roundup and glyphosate exposure on Japanese medaka (Oryzias latipes). *Aquat. Toxicol.* **2019**, *210*, 215−226.
(54) Ankley, G. T.; Jensen, K. M.; Kahl, M. D.; Korte, J. J.; Makynen, E. A. Description and evaluation of a short-term reproduction test with the fathead minnow (Pimephales promelas). *Environ. Toxicol. Chem., Int. J.* **2001**, *20*, 1276−1290.
(55) Migliaccio, M.; Chioccarelli, T.; Ambrosino, C.; Suglia, A.; Manfrevola, F.; Carnevali, O.; Fasano, S.; Pierantoni, R.; Cobellis, G. Characterization of Follicular Atresia Responsive to BPA in Zebrafish by Morphometric Analysis of Follicular Stage Progression. *Int. J. Endocrinol.* **2018**, *2018*, 4298195.
(56) Selman, K.; Wallace, R. A.; Sarka, A.; Qi, X. Stages of oocyte development in the zebrafish, Brachydanio rerio. *J. Morphol.* **1993**, *218*, 203−224.
(57) Üçüncü, S. İ.; Cakici, O. Atresia and apoptosis in preovulatory follicles in the ovary of Danio rerio (zebrafish). *Turkish J. Fish. Aquat. Sci.* **2009**, *9* (), DOI: 10.4194/trjfas.2009.0214.
(58) Wang, X.; Hill, D.; Tillitt, D. E.; Bhandari, R. K. Bisphenol A and 17α-ethinylestradiol-induced transgenerational differences in expression of osmoregulatory genes in the gill of medaka (Oryzias latipes). *Aquat. Toxicol.* **2019**, *211*, 227−234.
(59) Aranda, P. S.; LaJoie, D. M.; Jorcyk, C. L. Bleach gel: a simple agarose gel for analyzing RNA quality. *Electrophoresis* **2012**, *33*, 366−369.
(60) Chen, S.; Zhou, Y.; Chen, Y.; Gu, J. fastp: an ultra-fast all-in-one FASTQ preprocessor. *Bioinformatics* **2018**, *34*, i884−i890.
(61) Dobin, A.; Davis, C. A.; Schlesinger, F.; Drenkow, J.; Zaleski, C.; Jha, S.; Batut, P.; Chaisson, M.; Gingeras, T. R. STAR: ultrafast universal RNA-seq aligner. *Bioinformatics* **2013**, *29*, 15−21.
(62) Love, M. I.; Anders, S.; Huber, W. Analyzing RNA-seq data with DESeq2. *Bioconductor* **2017**, *2*, 1−63.
(63) Subramanian, A.; Tamayo, P.; Mootha, V. K.; Mukherjee, S.; Ebert, B. L.; Gillette, M. A.; Paulovich, A.; Pomeroy, S. L.; Golub, T. R.; Lander, E. S.; Mesirov, J. P. Gene set enrichment analysis: a knowledge-based approach for interpreting genome-wide expression profiles. *Proc. Natl. Acad. Sci.* **2005**, *102*, 15545−15550.
(64) Mootha, V. K.; Lindgren, C. M.; Eriksson, K.-F.; Subramanian, A.; Sihag, S.; Lehar, J.; Puigserver, P.; Carlsson, E.; Ridderstråle, M.; Laurila, E.; Houstis, N.; Daly, M. J.; Patterson, N.; Mesirov, J. P.; Golub, T. R.; Tamayo, P.; Spiegelman, B.; Lander, E. S.; Hirschhorn, J. N.; Altshuler, D.; Groop, L. C. PGC-1α-responsive genes involved in oxidative phosphorylation are coordinately downregulated in human diabetes. *Nat. Genet.* **2003**, *34*, 267−273.
(65) Liberzon, A.; Birger, C.; Thorvaldsdóttir, H.; Ghandi, M.; Mesirov, J. P.; Tamayo, P. The Molecular Signatures Database (MSigDB) hallmark gene set collection. *Cell Syst.* **2015**, *1*, 417−425.
(66) Aydos, A.; Gurel, A.; Oztemur Islakoglu, Y.; Noyan, S.; Gokce, B.; Ecemis, T.; Kaya, C.; Aksu, A. T.; Gur Dedeoglu, B. Identification of polycystic ovary syndrome (PCOS) specific genes in cumulus and mural granulosa cells. *PLoS One* **2016**, *11*, No. e0168875.
(67) Kaur, S.; Archer, K. J.; Devi, M. G.; Kriplani, A.; Strauss, J. F., III; Singh, R. Differential gene expression in granulosa cells from polycystic ovary syndrome patients with and without insulin resistance: identification of susceptibility gene sets through network analysis. *J. Clin. Endocrinol. Metab.* **2012**, *97*, E2016−E2021.
(68) Grøndahl, M. L.; Andersen, C. Y.; Bogstad, J.; Borgbo, T.; Hartvig Boujida, V.; Borup, R. Specific genes are selectively expressed between cumulus and granulosa cells from individual human pre-ovulatory follicles. *Mol. Hum. Reprod.* **2012**, *18*, 572−584.
(69) Lemecha, M.; Chalise, J. P.; Takamuku, Y.; Zhang, G.; Yamakawa, T.; Larson, G.; Itakura, K. Lcn2 mediates adipocyte-muscle-tumor communication and hypothermia in pancreatic cancer cachexia. *Mol. Metab.* **2022**, *66*, No. 101612.
(70) Cleary, J. A.; Tillitt, D. E.; Vom Saal, F. S.; Nicks, D. K.; Claunch, R. A.; Bhandari, R. K. Atrazine induced transgenerational reproductive effects in medaka (Oryzias latipes). *Environ. Pollut.* **2019**, *251*, 639−650.
(71) Untergasser, A.; Cutcutache, I.; Koressaar, T.; Ye, J.; Faircloth, B. C.; Remm, M.; Rozen, S. G. Primer3–new capabilities and interfaces. *Nucleic Acids Res.* **2012**, *40*, No. e115.
(72) Raudvere, U.; Kolberg, L.; Kuzmin, I.; Arak, T.; Adler, P.; Peterson, H.; Vilo, J. g: Profiler: a web server for functional enrichment analysis and conversions of gene lists (2019 update). *Nucleic Acids Res.* **2019**, *47*, W191−W198.
(73) Tian, Y.; Xu, T.; Li, Y.; Liu, Y.; Liu, J. An untargeted LC-MS metabolomics approach to the metabolic profiles of bottom cultured scallops (Mizuhopecten yessoensis) subjected to mechanical shock in early post-harvest handling. *Aquaculture* **2021**, *533*, No. 736061.
(74) Jones, D. D., Jr.; Caesar, L. K.; Pelzer, C. V.; Crandall, W. J.; Jenul, C.; Todd, D. A.; Horswill, A. R.; Cech, N. B. Targeted and untargeted analysis of secondary metabolites to monitor growth and quorum sensing inhibition for methicillin-resistant Staphylococcus aureus (MRSA). *J. Microbiol. Methods* **2020**, *176*, No. 106000.
(75) Chong, J.; Soufan, O.; Li, C.; Caraus, I.; Li, S.; Bourque, G.; Wishart, D. S.; Xia, J. MetaboAnalyst 4.0: towards more transparent and integrative metabolomics analysis. *Nucleic Acids Res.* **2018**, *46*, W486−W494.
(76) Wishart, D. S.; Tzur, D.; Knox, C.; Eisner, R.; Guo, A. C.; Young, N.; Cheng, D.; Jewell, K.; Arndt, D.; Sawhney, S.; Fung, C.; Nikolai, L.; Lewis, M.; Coutouly, M.-A.; Forsythe, I.; Tang, P.; Shrivastava, S.; Jeroncic, K.; Stothard, P.; Amegbey, G.; Block, D.; Hau, D. D.; Wagner, J.; Miniaci, J.; Clements, M.; Gebremedhin, M.; Guo, N.; Zhang, Y.; Duggan, G. E.; MacInnis, G. D.; Weljie, A. M.; Dowlatabadi, R.; Bamforth, F.; Clive, D.; Greiner, R.; Li, L.; Marrie, T.; Sykes, B. D.; Vogel, H. J.; Querengesser, L. HMDB: the Human Metabolome Database. *Nucleic Acids Res.* **2007**, *35*, D521−D526.
(77) Smith, C. A.; Maille, G. O.; Want, E. J.; Qin, C.; Trauger, S. A.; Brandon, T. R.; Custodio, D. E.; Abagyan, R.; Siuzdak, G. METLIN: A Metabolite Mass Spectral Database. *Ther. Drug Monit.* **2005**, *27*, 747.
(78) Ladisa, C.; Ma, Y.; Habibi, H. R. Seasonally related metabolic changes and energy allocation associated with growth and reproductive phases in the liver of male goldfish (Carassius auratus). *J. Proteomics* **2021**, *241*, No. 104237.
(79) He, Z.; Liu, Z.; Gong, L. Biomarker identification and pathway analysis of rheumatoid arthritis based on metabolomics in combination with ingenuity pathway analysis. *Proteomics* **2021**, *21*, 2100037.
(80) Ma, Z.; Li, Z.; Wang, H.; Wang, R.; Han, X. Screening of serum oxysterol biomarkers for colon cancer by liquid chromatography-tandem mass spectrometry. *Se p'u Chin. J. Chromatogr.* **2022**, *40*, 541−546.
(81) Rajska, A.; Buszewska-Forajta, M.; Rachoń, D.; Markuszewski, M. J. Metabolomic Insight into Polycystic Ovary Syndrome-An Overview. *Int. J. Mol. Sci.* **2020**, *21*, 4853.

(82) Zhao, Y.; Fu, L.; Li, R.; Wang, L.-N.; Yang, Y.; Liu, N.-N.; Zhang, C.-M.; Wang, Y.; Liu, P.; Tu, B.-B.; Zhang, X.; Qiao, J. Metabolic profiles characterizing different phenotypes of polycystic ovary syndrome: plasma metabolomics analysis. *BMC Med.* **2012**, *10*, 153.
(83) Kramer, A.; Green, J.; Pollard, J., Jr.; Tugendreich, S. Causal analysis approaches in Ingenuity Pathway Analysis. *Bioinformatics* **2014**, *30*, 523−530.
(84) Wang, Z.; Ma, P.; Wang, Y.; Hou, B.; Zhou, C.; Tian, H.; Li, B.; Shui, G.; Yang, X.; Qiang, G.; Yin, C.; Du, G. Untargeted metabolomics and transcriptomics identified glutathione metabolism disturbance and PCS and TMAO as potential biomarkers for ER stress in lung. *Sci. Rep.* **2021**, *11*, 14680.
(85) Legro, R. S. POLYCYSTIC OVARY SYNDROME: Phenotype to Genotype. *Endocrinol. Metab. Clin. North Am.* **1999**, *28*, 379−396.
(86) McAllister, J. M.; Legro, R. S.; Modi, B. P.; Strauss, J. F. Functional genomics of PCOS: from GWAS to molecular mechanisms. *Trends Endocrinol. Metab.* **2015**, *26*, 118−124.
(87) Gorsic, L. K.; Kosova, G.; Werstein, B.; Sisk, R.; Legro, R. S.; Hayes, M. G.; Teixeira, J. M.; Dunaif, A.; Urbanek, M. Pathogenic Anti-Müllerian Hormone Variants in Polycystic Ovary Syndrome. *J. Clin. Endocrinol. Metab.* **2017**, *102*, 2862−2872.
(88) Azziz, R. Erratum: PCOS in 2016: New insights into the genetics of polycystic ovary syndrome. *Nat. Rev. Endocrinol.* **2016**, *12*, 183−183.
(89) Nilsson, E. E.; Ben Maamar, M.; Skinner, M. K. Role of epigenetic transgenerational inheritance in generational toxicology. *Environ. Epigenet.* **2022**, *8*, dvac001.
(90) Nilsson, E. E.; Sadler-Riggleman, I.; Skinner, M. K. Environmentally induced epigenetic transgenerational inheritance of disease. *Environ. Epigenet.* **2018**, *4*, dvy016.
(91) Skinner, M. K.; Haque, C. G.-B. M.; Nilsson, E.; Bhandari, R.; McCarrey, J. R. Environmentally induced transgenerational epigenetic reprogramming of primordial germ cells and the subsequent germ line. *PLoS One* **2013**, *8*, No. e66318.
(92) van Esterik, J. C. J.; Dollé, M. E. T.; Lamoree, M. H.; van Leeuwen, S. P. J.; Hamers, T.; Legler, J.; van der Ven, L. T. M. Programming of metabolic effects in C57BL/6JxFVB mice by exposure to bisphenol A during gestation and lactation. *Toxicology* **2014**, *321*, 40−52.
(93) Malaisé, Y.; Menard, S.; Cartier, C.; Gaultier, E.; Lasserre, F.; Lencina, C.; Harkat, C.; Geoffre, N.; Lakhal, L.; Castan, I.; Olier, M.; Houdeau, E.; Guzylack-Piriou, L. Gut dysbiosis and impairment of immune system homeostasis in perinatally-exposed mice to Bisphenol A precede obese phenotype development. *Sci. Rep.* **2017**, *7*, 14472.
(94) Fernández, M.; Bourguignon, N.; Lux-Lantos, V.; Libertun, C. Neonatal exposure to bisphenol a and reproductive and endocrine alterations resembling the polycystic ovarian syndrome in adult rats. *Environ. Health Perspect.* **2010**, *118*, 1217−1222.
(95) Zhou, W.; Fang, F.; Zhu, W.; Chen, Z.-J.; Du, Y.; Zhang, J. Bisphenol A and ovarian reserve among infertile women with polycystic ovarian syndrome. *Int. J. Environ. Res. Public Health* **2017**, *14*, 18.
(96) Legeay, S.; Faure, S. Is bisphenol A an environmental obesogen? *Fundam. Clin. Pharmacol.* **2017**, *31*, 594−609.
(97) Ahmed, S.; Atlas, E. Bisphenol S-and bisphenol A-induced adipogenesis of murine preadipocytes occurs through direct peroxisome proliferator-activated receptor gamma activation. *Int. J. Obes.* **2016**, *40*, 1566−1573.
(98) De Filippis, E.; Li, T.; Rosen, E. D. Exposure of adipocytes to bisphenol-A in vitro interferes with insulin action without enhancing adipogenesis. *PLoS One* **2018**, *13*, No. e0201122.
(99) Hugo, E. R.; Brandebourg, T. D.; Woo, J. G.; Loftus, J.; Alexander, J. W.; Ben-Jonathan, N. Bisphenol A at Environmentally Relevant Doses Inhibits Adiponectin Release from Human Adipose Tissue Explants and Adipocytes. *Environ. Health Perspect.* **2008**, *116*, 1642−1647.
(100) Grasselli, E.; Cortese, K.; Voci, A.; Vergani, L.; Fabbri, R.; Barmo, C.; Gallo, G.; Canesi, L. Direct effects of Bisphenol A on lipid homeostasis in rat hepatoma cells. *Chemosphere* **2013**, *91*, 1123−1129.
(101) Chourasia, T. K.; Joy, K. P. Estrogen-2/4-hydroxylase activity is stimulated during germinal vesicle breakdown induced by hCG, IGF-1, GH and insulin in the catfish Heteropneustes fossilis. *Gen. Comp. Endocrinol.* **2008**, *155*, 413−421.
(102) Diamanti-Kandarakis, E.; Christakou, C. D. Insulin resistance in PCOS. *Diagn. Manage. Polycystic Ovary Syndr.* **2009**, 35−61.
(103) Barreca, A.; Del Monte, P.; Ponzani, P.; Artini, P. G.; Genazzani, A. R.; Minuto, F. Intrafollicular insulin-like growth factor-II levels in normally ovulating women and in patients with polycystic ovary syndrome. *Fertil. Steril.* **1996**, *65*, 739−745.
(104) SAMOTO, T.; MARUO, T.; MATSUO, H.; KATAYAMA, K.; BARNEA, E. R.; MOCHIZUKI, M. Altered expression of insulin and insulin-like growth factor-I receptors in follicular and stromal compartments of polycystic ovaries. *Endocr. J.* **1993**, *40*, 413−424.
(105) Lewandowski, K. C.; Cajdler-Łuba, A.; Salata, I.; Bieńkiewicz, M.; Lewiński, A. The utility of the gonadotrophin releasing hormone (GnRH) test in the diagnosis of polycystic ovary syndrome (PCOS). *Endokrynol. Pol.* **2011**, *62*, 120−128.
(106) Tuan Nguyen, A.; Chia, J. H. Z.; Kazeto, Y.; Wylie, M. J.; Mark Lokman, P. Induction of oocyte development in previtellogenic eel, *Anguilla australis*. *Gen. Comp. Endocrinol.* **2020**, *291*, No. 113404.
(107) Martyniuk, C. J.; Kroll, K. J.; Porak, W. F.; Steward, C.; Grier, H. J.; Denslow, N. D. Seasonal relationship between gonadotropin, growth hormone, and estrogen receptor mRNA expression in the pituitary gland of largemouth bass. *Gen. Comp. Endocrinol.* **2009**, *163*, 306−317.
(108) Li, Y.; Wei, L.; Xiong, Y.; Liang, X. Effect of luteinizing hormone vs follicular stimulating hormone ratio on anti-Müllerian hormone secretion and folliculogenesis in patients with polycystic ovarian syndrome. *Zhonghua Fuchanke Zazhi* **2010**, *45*, 567−570.
(109) Campbell, B.; Dickey, J.; Beckman, B.; Young, G.; Pierce, A.; Fukada, H.; Swanson, P. Previtellogenic oocyte growth in salmon: relationships among body growth, plasma insulin-like growth factor-1, estradiol-17beta, follicle-stimulating hormone and expression of ovarian genes for insulin-like growth factors, steroidogenic-acute regulatory protein and receptors for gonadotropins, growth hormone, and somatolactin. *Biol. Reprod.* **2006**, *75*, 34−44.
(110) Luckenbach, J. A.; Iliev, D. B.; Goetz, F. W.; Swanson, P. Identification of differentially expressed ovarian genes during primary and early secondary oocyte growth in coho salmon. *Reprod. Biol. Endocrinol.* **2008**, *6*, 2.
(111) Zhang, Z.; Lau, S. W.; Zhang, L.; Ge, W. Disruption of Zebrafish Follicle-Stimulating Hormone Receptor (fshr) But Not Luteinizing Hormone Receptor (lhcgr) Gene by TALEN Leads to Failed Follicle Activation in Females Followed by Sexual Reversal to Males. *Endocrinology* **2015**, *156*, 3747−3762.
(112) Homburg, R.; Crawford, G. The role of AMH in anovulation associated with PCOS: a hypothesis. *Hum. Reprod.* **2014**, *29*, 1117−1121.
(113) Yang, Z.; Shi, J.; Guo, Z.; Chen, M.; Wang, C.; He, C.; Zuo, Z. A pilot study on polycystic ovarian syndrome caused by neonatal exposure to tributyltin and bisphenol A in rats. *Chemosphere* **2019**, *231*, 151−160.
(114) Ijaz, S.; Ullah, A.; Shaheen, G.; Jahan, S. Exposure of BPA and its alternatives like BPB, BPF, and BPS impair subsequent reproductive potentials in adult female Sprague Dawley rats. *Toxicol. Mech. Methods* **2020**, *30*, 60−72.
(115) Gámez, J. M.; Penalba, R.; Cardoso, N.; Bernasconi, P. S.; Carbone, S.; Ponzo, O.; Pandolfi, M.; Scacchi, P.; Reynoso, R. Exposure to a low dose of bisphenol A impairs pituitary-ovarian axis in prepubertal rats: Effects on early folliculogenesis. *Environ. Toxicol. Pharmacol.* **2015**, *39*, 9−15.
(116) Rutkowska, A.; Rachoń, D. Bisphenol A (BPA) and its potential role in the pathogenesis of the polycystic ovary syndrome (PCOS). *Gynecol. Endocrinol.* **2014**, *30*, 260−265.
(117) Björntorp, P. The regulation of adipose tissue distribution in humans. *Int. J. Obes. Relat. Metab. Disord.* **1996**, *20*, 291−302.

https://doi.org/10.1021/acs.est.3c01922
Environ. Sci. Technol. 2023, 57, 12602−12619

(118) Krishnan, A.; Muthusami, S. Hormonal alterations in PCOS and its influence on bone metabolism. *J. Endocrinol.* **2017**, *232*, R99−R113.
(119) Xu, J.-N.; Zeng, C.; Zhou, Y.; Peng, C.; Zhou, Y.-F.; Xue, Q. Metformin Inhibits StAR Expression in Human Endometriotic Stromal Cells via AMPK-Mediated Disruption of CREB-CRTC2 Complex Formation. *J. Clin. Endocrinol. Metab.* **2014**, *99*, 2795−2803.
(120) Sands, W. A.; Palmer, T. M. Regulating gene transcription in response to cyclic AMP elevation. *Cell. Signalling* **2008**, *20*, 460−466.
(121) Knight, P. G.; Glister, C. Local roles of TGF-β superfamily members in the control of ovarian follicle development. *Anim. Reprod. Sci.* **2003**, *78*, 165−183.
(122) Diamanti-Kandarakis, E.; Dunaif, A. Insulin Resistance and the Polycystic Ovary Syndrome Revisited: An Update on Mechanisms and Implications. *Endocr. Rev.* **2012**, *33*, 981−1030.
(123) Huang, L.; Wang, H. Y.; Li, J. D.; Wang, J. H.; Zhou, Y.; Luo, R. Z.; Yun, J. P.; Zhang, Y.; Jia, W. H.; Zheng, M. KPNA2 promotes cell proliferation and tumorigenicity in epithelial ovarian carcinoma through upregulation of c-Myc and downregulation of FOXO3a. *Cell Death Dis.* **2013**, *4*, e745−e745.
(124) Johnson, K.; Choi, Y.; DeGroot, E.; Samuels, I.; Creasey, A.; Aarden, L. Potential mechanisms for a proinflammatory vascular cytokine response to coagulation activation. *J. Immunol.* **1998**, *160*, 5130−5135.
(125) Vivanco, I.; Sawyers, C. L. The phosphatidylinositol 3-kinase−AKT pathway in human cancer. *Nat. Rev. Cancer* **2002**, *2*, 489−501.
(126) Altomare, D. A.; Wang, H. Q.; Skele, K. L.; Rienzo, A. D.; Klein-Szanto, A. J.; Godwin, A. K.; Testa, J. R. AKT and mTOR phosphorylation is frequently detected in ovarian cancer and can be targeted to disrupt ovarian tumor cell growth. *Oncogene* **2004**, *23*, 5853−5857.
(127) Bornstein, S.; White, R.; Malkoski, S.; Oka, M.; Han, G.; Cleaver, T.; Reh, D.; Andersen, P.; Gross, N.; Olson, S.; Deng, C.; Lu, S. L.; Wang, X. J. Smad4 loss in mice causes spontaneous head and neck cancer with increased genomic instability and inflammation. *J. Clin. Invest.* **2009**, *119*, 3408−3419.
(128) Riese, C.; Michaelis, M.; Mentrup, B.; Götz, F.; Köhrle, J.; Schweizer, U.; Schomburg, L. Selenium-dependent pre-and post-transcriptional mechanisms are responsible for sexual dimorphic expression of selenoproteins in murine tissues. *Endocrinology* **2006**, *147*, 5883−5892.
(129) Wang, L.; Fan, H.; Zou, Y.; Yuan, Q.; Hu, X.; Chen, X.; Zhu, C.; Zhang, X.; Cui, H. Aberrant expression of long non-coding RNAs in exosomes in follicle fluid from PCOS patients. *Front. Genet.* **2021**, *11*, No. 608178.
(130) Han, I.; Jeong, S.-J.; Lee, H.-J.; Koh, W.; Lee, H.-J.; Lee, E.-O.; Kim, H. S.; Lee, S. J.; Chen, C.-Y.; Jung, M.-H.; Kim, S.-H. Proteomic analysis of mesenchymal stem-like cells derived from ovarian teratoma: Potential role of glutathione S-transferase M2 in ovarian teratoma. *Proteomics* **2011**, *11*, 352−360.
(131) Duggavathi, R.; Siddappa, D.; Schuermann, Y.; Pansera, M.; Menard, I. J.; Praslickova, D.; Agellon, L. B. The fatty acid binding protein 6 gene (Fabp6) is expressed in murine granulosa cells and is involved in ovulatory response to superstimulation. *J. Reprod. Dev.* **2015**, *61*, 237−240.
(132) Tamura, R.; Nakaoka, H.; Yoshihara, K.; Mori, Y.; Yachida, N.; Nishikawa, N.; Motoyama, T.; Okuda, S.; Inoue, I.; Enomoto, T. Novel MXD4−NUTM1 fusion transcript identified in primary ovarian undifferentiated small round cell sarcoma. *Genes, Chromosomes Cancer* **2018**, *57*, 557−563.
(133) Lee, T. I.; Young, R. A. Transcriptional regulation and its misregulation in disease. *Cell* **2013**, *152*, 1237−1251.
(134) Kuang, Y.; Lu, F.; Guo, J.; Xu, H.; Wang, Q.; Xu, C.; Zeng, L.; Yi, S. Histone demethylase KDM2B upregulates histone methyltransferase EZH2 expression and contributes to the progression of ovarian cancer in vitro and in vivo. *OncoTargets Ther.* **2017**, *10*, 3131.
(135) Hayashi, A.; Horiuchi, A.; Kikuchi, N.; Hayashi, T.; Fuseya, C.; Suzuki, A.; Konishi, I.; Shiozawa, T. Type-specific roles of histone deacetylase (HDAC) overexpression in ovarian carcinoma: HDAC1 enhances cell proliferation and HDAC3 stimulates cell migration with downregulation of E-cadherin. *Int. J. Cancer* **2010**, *127*, 1332−1346.
(136) Chusri, P.; Kumthip, K.; Hong, J.; Zhu, C.; Duan, X.; Jilg, N.; Fusco, D. N.; Brisac, C.; Schaefer, E. A.; Cai, D.; Peng, L. F.; Maneekarn, N.; Lin, W.; Chung, R. T. HCV induces transforming growth factor β1 through activation of endoplasmic reticulum stress and the unfolded protein response. *Sci. Rep.* **2016**, *6*, 1−13.
(137) Cheng, J.-C.; Chang, H.-M.; Fang, L.; Sun, Y.-P.; Leung, P. C. K. TGF-β1 up-regulates connective tissue growth factor expression in human granulosa cells through Smad and ERK1/2 signaling pathways. *PLoS One* **2015**, *10*, No. e0126532.
(138) Chang, H.-M.; Fang, Y.; Liu, P.-P.; Cheng, J.-C.; Yang, X.; Leung, P. C. K. Connective tissue growth factor mediates growth differentiation factor 8-induced increase of lysyl oxidase activity in human granulosa-lutein cells. *Mol. Cell. Endocrinol.* **2016**, *434*, 186−198.
(139) Lenna, S.; Trojanowska, M. The role of endoplasmic reticulum stress and the unfolded protein response in fibrosis. *Curr. Opin. Rheumatol.* **2012**, *24*, 663.
(140) Tanjore, H.; Lawson, W. E.; Blackwell, T. S. Endoplasmic reticulum stress as a pro-fibrotic stimulus. *Biochim. Biophys. Acta, Mol. Basis Dis.* **2013**, *1832*, 940−947.
(141) Hughesdon, P. Morphology and morphogenesis of the Stein-Leventhal ovary and of so-called″ hyperthecosis″. *Obstet. Gynecol. Surv.* **1982**, *37*, 59−77.
(142) Sumarac-Dumanovic, M.; Apostolovic, M.; Janjetovic, K.; Jeremic, D.; Popadic, D.; Ljubic, A.; Micic, J.; Dukanac-Stamenkovic, J.; Tubic, A.; Stevanovic, D.; Micic, D.; Trajkovic, V. Downregulation of autophagy gene expression in endometria from women with polycystic ovary syndrome. *Mol. Cell. Endocrinol.* **2017**, *440*, 116−124.
(143) Kumariya, S.; Ubba, V.; Jha, R. K.; Gayen, J. R. Autophagy in ovary and polycystic ovary syndrome: role, dispute and future perspective. *Autophagy* **2021**, *17*, 2706−2733.
(144) Salehi, E.; Aflatoonian, R.; Moeini, A.; Yamini, N.; Asadi, E.; Khosravizadeh, Z.; Tarzjani, M. D.; harat, Z. N.; Abolhassani, F. Apoptotic biomarkers in cumulus cells in relation to embryo quality in polycystic ovary syndrome. *Arch. Gynecol. Obstet.* **2017**, *296*, 1219−1227.
(145) Moon, M. K.; Kim, M. J.; Jung, I. K.; Do Koo, Y.; Ann, H. Y.; Lee, K. J.; Kim, S. H.; Yoon, Y. C.; Cho, B.-J.; Park, K. S.; Jang, H. C.; Park, Y. J. Bisphenol A impairs mitochondrial function in the liver at doses below the no observed adverse effect level. *J. Korean Med. Sci.* **2012**, *27*, 644−652.
(146) Cree-Green, M.; Carreau, A.-M.; Rahat, H.; Garcia-Reyes, Y.; Bergman, B. C.; Pyle, L.; Nadeau, K. J. Amino acid and fatty acid metabolomic profile during fasting and hyperinsulinemia in girls with polycystic ovarian syndrome. *Am. J. Physiol.: Endocrinol. Metab.* **2019**, *316*, E707−E718.
(147) Newgard, C. B.; An, J.; Bain, J. R.; Muehlbauer, M. J.; Stevens, R. D.; Lien, L. F.; Haqq, A. M.; Shah, S. H.; Arlotto, M.; Slentz, C. A.; Rochon, J.; Gallup, D.; Ilkayeva, O.; Wenner, B. R.; Yancy, W. S., Jr.; Eisenson, H.; Musante, G.; Surwit, R. S.; Millington, D. S.; Butler, M. D.; Svetkey, L. P. A branched-chain amino acid-related metabolic signature that differentiates obese and lean humans and contributes to insulin resistance. *Cell Metab.* **2009**, *9*, 311−326.
(148) Adams, S. H. Emerging perspectives on essential amino acid metabolism in obesity and the insulin-resistant state. *Adv. Nutr.* **2011**, *2*, 445−456.
(149) Krishna, M. B.; Joseph, A.; Thomas, P. L.; Dsilva, B.; Pillai, S. M.; Laloraya, M. Impaired arginine metabolism coupled to a defective redox conduit contributes to low plasma nitric oxide in polycystic ovary syndrome. *Cell. Physiol. Biochem.* **2018**, *43*, 1880−1892.
(150) Zhang, Z.; Hong, Y.; Chen, M.; Tan, N.; Liu, S.; Nie, X.; Zhou, W. Serum metabolomics reveals metabolic profiling for women with hyperandrogenism and insulin resistance in polycystic ovary syndrome. *Metabolomics* **2020**, *16*, 20.
(151) RoyChoudhury, S.; More, T. H.; Chattopadhyay, R.; Lodh, I.; Ray, C. D.; Bose, G.; Sarkar, H. S.; Chakravarty, B.; Rapole, S.; Chaudhury, K. Polycystic ovary syndrome in Indian women: a mass

spectrometry based serum metabolomics approach. *Metabolomics* **2017**, *13*, 115.
(152) Zhao, X.; Feng, X.; Zhao, X.; Jiang, Y.; Li, X.; Niu, J.; Meng, X.; Wu, J.; Xu, G.; Hou, L. How to Screen and Prevent Metabolic Syndrome in Patients of PCOS Early: Implications From Metabolomics. *Front. Endocrinol.* **2021**, *2*, No. 659268.
(153) Tian, J.; Xu, Y.; Xiong, Y.; Zuo, L.; Zhou, M.; Cao, C.; Huang, X.; Wang, J. Metabolomics combined with network pharmacology to explore the mechanisms of modified Guishen pill to ameliorate polycystic ovary syndrome. *Comput. Biol. Med.* **2022**, *148*, No. 105790.
(154) Huang, W.; Li, S.; Luo, N.; Lu, K.; Ban, S.; Lin, H. Dynamic analysis of the biochemical changes in rats with polycystic ovary syndrome (PCOS) using urinary 1H NMR-based metabonomics. *Horm. Metab. Res.* **2020**, *52*, 49−57.
(155) Zhang, B.; Shen, S.; Gu, T.; Hong, T.; Liu, J.; Sun, J.; Wang, H.; Bi, Y.; Zhu, D. Increased circulating conjugated primary bile acids are associated with hyperandrogenism in women with polycystic ovary syndrome. *J. Steroid Biochem. Mol. Biol.* **2019**, *189*, 171−175.
(156) Karadeniz, M.; Erdoğan, M.; Ayhan, Z.; Yalcın, M.; Olukman, M.; Cetinkalp, S.; Alper, G. E.; Eroglu, Z.; Tetik, A.; Cetintas, V.; Ozgen, A. G.; Saygılı, F.; Yılmaz, C. Effect Of G2706A and G1051A polymorphisms of the ABCA1 gene on the lipid, oxidative stress and homocystein levels in Turkish patients with polycystıc ovary syndrome. *Lipids Health Dis.* **2011**, *10*, 193.
(157) Monir, R.; Badawy, A.; Mokhtar, N.; Nabil, H.; Alruwaili, M. ABCA1 gene polymorphism and oxidative stress in polycystic ovary syndrome: Role of antioxidant therapy for prevention and control. *Bull. Egypt. Soc.Physiol. Sci.* **2017**, *37*, 143−153.
(158) Chen, J.; Zhou, Q.; Zhang, Y.; Tan, W.; Gao, H.; Zhou, L.; Xiao, S.; Gao, J.; Li, J.; Zhu, Z. Discovery of novel serum metabolic biomarkers in patients with polycystic ovarian syndrome and premature ovarian failure. *Bioengineered* **2021**, *12*, 8778−8792.
(159) Gutmann, D. H.; Saporito-Irwin, S.; DeClue, J. E.; Wienecke, R.; Guha, A. Alterations in the rap1 signaling pathway are common in human gliomas. *Oncogene* **1997**, *15*, 1611−1616.
(160) Ramasamy, R.; Yan, S. F.; Schmidt, A. M. Receptor for AGE (RAGE): signaling mechanisms in the pathogenesis of diabetes and its complications. *Ann. N. Y. Acad. Sci.* **2011**, *1243*, 88−102.
(161) Diamanti-Kandarakis, E.; Argyrakopoulou, G.; Economou, F.; Kandaraki, E.; Koutsilieris, M. Defects in insulin signaling pathways in ovarian steroidogenesis and other tissues in polycystic ovary syndrome (PCOS). *J. Steroid Biochem. Mol. Biol.* **2008**, *109*, 242−246.
(162) Mihanfar, A.; Nouri, M.; Roshangar, L.; Khadem-Ansari, M. H. Therapeutic potential of quercetin in an animal model of PCOS: Possible involvement of AMPK/SIRT-1 axis. *Eur. J. Pharmacol.* **2021**, *900*, No. 174062.
(163) Templehof, H.; Moshe, N.; Avraham-Davidi, I.; Yaniv, K. Zebrafish mutants provide insights into Apolipoprotein B functions during embryonic development and pathological conditions. *JCI Insight* **2021**, *6*, No. e7130399.
(164) Qu, X.; Donnelly, R. Sex Hormone-Binding Globulin (SHBG) as an Early Biomarker and Therapeutic Target in Polycystic Ovary Syndrome. *Int. J. Mol. Sci.* **2020**, *21*, 8191.
(165) Christensen, S. B.; Black, M. H.; Smith, N.; Martinez, M. M.; Jacobsen, S. J.; Porter, A. H.; Koebnick, C. Prevalence of polycystic ovary syndrome in adolescents. *Fertil. Steril.* **2013**, *100*, 470−477.
(166) De Leo, V.; Di Sabatino, A.; Musacchio, M. C.; Morgante, G.; Scolaro, V.; Cianci, A.; Petraglia, F. Effect of oral contraceptives on markers of hyperandrogenism and SHBG in women with polycystic ovary syndrome. *Contraception* **2010**, *82*, 276−280.
(167) Tata, J. R.; Smith, D. F. Vitellogenesis: A Versatile Model for Hormonal Regulation of Gene Expression. In *Proceedings of the 1978 Laurentian Hormone Conference*, Greep, R. O. Ed. Academic Press: Boston, 1979; Vol. *35*, pp. 47−95, DOI: 10.1016/B978-0-12-571135-7.50006-0.
(168) Nagahama, Y. Endocrine regulation of gametogenesis in fish. International. *J. Dev. Biol.* **1994**, *38*, 217−229.

https://doi.org/10.1021/acs.est.3c01922
Environ. Sci. Technol. 2023, 57, 12602−12619